Adsorption (2019) 25:1437–1474
https://doi.org/10.1007/s10450-019-00155-w

INVITED REVIEW ARTICLE

Medical oxygen concentrators: a review of progress in air separation technology

Mark W. Ackley[1]

Received: 16 May 2019 / Revised: 15 July 2019 / Accepted: 19 July 2019 / Published online: 14 August 2019

Abstract

Air separation by adsorption to produce oxygen for industrial and medical applications represents one of several important commercialized adsorption processes. Fueled by the introduction of synthetic zeolites, adsorbent and process development for air separation have progressed steadily over the last five decades. Early progress was driven primarily by large-scale industrial applications, however, small-scale medical oxygen concentrators (MOC) soon followed. This review presents an overview of the various types of commercially available MOCs, as well as the underlying adsorption technology. Key developments and essential concepts are summarized for air separation technology as it applies to both large and small-scale systems. Specific research targeting oxygen concentrators is also reviewed. The introduction of pulse flow oxygen conserving methodology has given rise to portable concentrators. Pulse flow represents not only a disruptive technology for the small-scale medical products, but also introduces operational challenges not present in large-scale industrial air separation. Process intensification utilizing small adsorbent particles and fast cycles is reviewed along with other key developments in air separation that apply to both large and small-scale systems. Challenges to further improvements in the medical concentrators are explored and opportunities for future research are identified.

Keywords Air separation · Medical oxygen concentrator · Portable oxygen concentrator · LiX adsorbents · Pressure swing adsorption · Intensification

Contents

Mark W. Ackley: Retired (Praxair, Inc.).

✉ Mark W. Ackley
ackleymw@verizon.net

[1] East Aurora, NY, USA

1 Introduction

Oxygen for industrial and medical applications is produced by separating air by either cryogenic distillation or by ambient temperature pressure swing adsorption (PSA) using nitrogen-selective zeolites. Oxygen purity is typically 99 + % from the former and 90 ± 5% from the latter. PSA air separation (Skarstrom 1960) became practical and economically feasible with the development of synthetic molecular sieves (Milton 1959). Motivation for developing PSA air separation was provided by large scale industrial applications that could capture significant cost benefits by replacing air with 90% O_2, e.g. waste water treatment, steel making, pulp and paper production, etc. (Reiss 1994). Such benefits included the elimination of waste nitrogen and the associated energy losses incurred by using air in high temperature processes, or alternatively capturing the savings of the lower cost of lower purity O_2 in processes that had been using high purity O_2. Industrial scale O_2 production by PSA is limited to < 300 tons per day O_2 (TPDO) for single-train air separation plants, while cryogenic air separation plants as large as 3000 TPDO are currently in operation.

The development of small-scale oxygen concentrators for use in individual patient long term oxygen therapy (LTOT) soon followed the introduction of industrial scale adsorptive air separation, with the first O_2 concentrators appearing in the early to mid-1970s (Cotes et al. 1969; Cassidy and Holmes 1984). These concentrators were based upon the same PSA process and N_2-selective zeolite technologies as the larger scale units, but with significantly lower O_2 production rates, e.g. a concentrator producing 5 lpm of 90% O_2 is equivalent to about 0.011 TPDO. Adsorbent and PSA process technology advancements in air separation have been largely driven by industrial scale O_2 production. Many of these improvements are directly applicable to small-scale concentrators, although there are some distinct differences related to scale when employing intensification methodologies. The purpose of this review is to examine adsorptive air separation development (past, present and future) relevant to MOCs.

It may be helpful to illuminate a few issues regarding terminology, with more in-depth explanations to follow. MOC is the general term used in this review to include all devices that concentrate O_2 from air by cyclic adsorption for personal medical use. Stationary concentrators are those devices intended for home use and are not easily transportable. Portable oxygen concentrators (POC) are smaller, lighter weight MOCs that can be transported by an individual patient for increased mobility and even during air travel. While some POCs can generate a continuous flow of O_2, pulse flow technology is the key ingredient to their smaller size. Figure 1 provides a block diagram differentiating the various means of providing O_2 to patients. Rapid pressure swing adsorption (RPSA) has been used to describe various air separation processes that are fundamentally different, leading to confusion in the published literature. This review intends to untangle this confusion.

Over the last two decades many studies on various aspects of "RPSA" air separation have been published. Coincidently during this same period there has been the introduction and proliferation of POCs. This development has had a significant impact upon LTOT—not all positive. A recent workshop of the American Thoracic Society (ATS) on Optimizing Home Oxygen Therapy (Jacobs et al 2018) declared "this ATS workshop confirmed a definable crisis in supplemental oxygen delivery in the United States…" While there are many factors contributing to these findings, e.g. medical reimbursement, competitive bid policies, education, etc., the variability in POC performance and the lack of funding for proper selection of equipment and monitoring of patient physiological response to using such equipment have also been identified as contributing factors.

Recent published evaluations of POC units have been predominantly performed by the medical community with the understandable emphasis upon the ability of various POC devices to effectively oxygenate patients according to

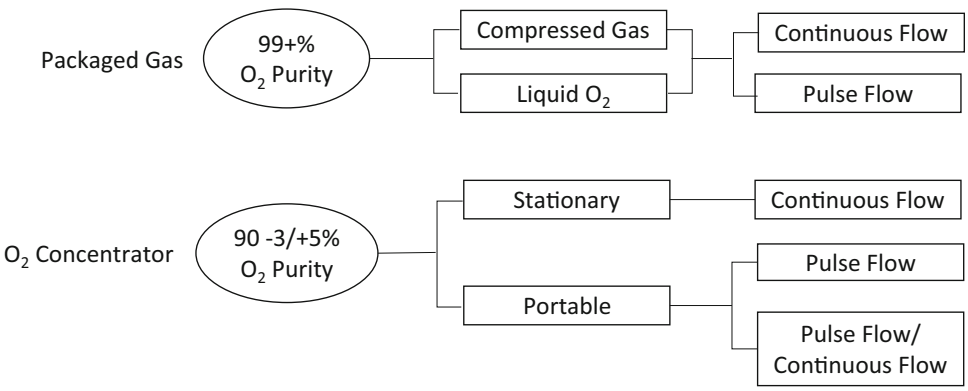

Fig. 1 Methods of delivery of oxygen for LTOT

their prescribed O_2 therapy. There are very few results in these studies that relate directly to the performance or key parameters of the PSA process within the POC unit, the notable exceptions being O_2 purity and the maximum O_2 production capacity or flow of the unit (also named minute volume in lpm). In contrast, published adsorption studies make little or no mention of the characteristics of breathing nor the specific requirements related to delivery of O_2 to the patient within the confines of the respiratory cycle. For these reasons, it is instructive to briefly review some of the key fundamentals of respiration and requirements for effective oxygen delivery.

2 Respiration and oxygen delivery

LTOT is the accepted protocol for treating patients with hypoxemia (deficient oxygenation of the blood). Such a condition results most notably from chronic obstructive pulmonary disease (COPD), although there are other respiratory disorders that also require LTOT. The aim of LTOT is to overcome this deficiency by supplementing the inspired air with high purity O_2 (typically $\geq 90\%$). The degree to which the inspired fraction of O_2 (F_{IO2}) is increased is directly related to the method of delivery of this supplemental O_2 (Tarpy and Celli 1995).

A set of baseline respiratory conditions are utilized here to facilitate the overall discussion—recognizing that respiration is dependent upon the individual, their level of activity and physiological condition. A typical breathing rate for a healthy adult at rest is 20 breaths per minute (br/min) with each breath consisting of an inspiration and expiration period. The inspiration period is approximately 1/3 of an individual breath cycle. Furthermore, air inspired during the first 60–70% of this inspiration period is most likely to reach the alveoli in the lung where useful exchange of O_2 and CO_2 with the gases in the blood occurs by diffusion. Air inspired in the latter stage of inhalation simply ends up in the dead space of the upper airways and is later exhaled without reaching the alveoli. Normal breathing in a healthy adult creates stable partial pressures of O_2 (P_{aO2}) and CO_2 (P_{aCO2}) in the arterial blood, with the P_{aCO2} level particularly critical to maintaining the pH of the blood.

Lower O_2 saturation levels of the blood occur in people experiencing hypoxemia. While the human body can compensate for these effects in the short term, long term effects are damaging to other parts of the body, e.g. heart, kidney, etc. (Tarpy and Celli 1995; Carlin et al. 2018). LTOT is aimed at mitigating these effects and restoring healthy O_2 saturation levels of the blood by providing supplemental O_2. Increasing the concentration and partial pressure of O_2 in the alveoli provides a greater driving force for O_2 diffusion resulting in higher O_2 saturation levels in the blood. During inspiration the patient breathes in air along with the supplemental O_2—typically delivered via a nasal cannula. Depending upon the source of supplemental O_2, the O_2 flow rate (or pulse dose) and the patient respiratory rate, the F_{IO2} may be increased from about 21% (air only) to as high as 40–45%. Typical F_{IO2} may range from about 25 to 35% for many POCs. The dilution of the high purity supplemental O_2 to these F_{IO2} levels is the result of the tidal volume (volume of gas exchanged between inspiration and exhalation, nominally about 500 ml), dead space, flow rate of supplemental O_2, respiratory rate and the concentration of gas in the anatomic reservoir at the end of exhalation (McCoy 2000). F_{IO2} is a key parameter in the assessment of various O_2 supply equipment and delivery methods. However, direct measurement of patient O_2 saturation levels by oximetry or O_2 blood saturation levels is the most direct means of determining whether or not the patient is receiving adequate oxygenation.

3 Overview of commercial medical oxygen concentrators

Prior to the introduction of O_2 concentrators for medical applications, in-home LTOT was provided from packaged gas oxygen, i.e. oxygen separated from air by cryogenic distillation and packaged as a high pressure compressed cylinder gas or as liquid oxygen (LOX) as illustrated in Fig. 1. This source of O_2 is also typical as bulk supply for use in hospitals. McCoy (2013) provides a good summary of the "evolution of home oxygen equipment."

Oxygen for medical use is considered to be a drug and must be prescribed by a physician (Dunne 2009). A typical prescription for the patient specifies flow rates (lpm) for different levels of activity and sleep. Such O_2 prescriptions generally refer to continuous flow rates of oxygen and are based upon historical data and experience in LTOT treatment of patients having various degrees of respiratory distress. Nevertheless, the effectiveness of the prescription needs to be verified via oximetry to determine the patient's oxygenation levels during activity, rest and sleep. Although not shown explicitly in Fig. 1, smaller (portable) packaged gas units are available for patient use outside the home. Cylinder gas products tend to be bulky and LOX systems are costly—both must be replenished.

Continuous flow LTOT treatment results in as much as 60–85% of the supplemental O_2 being wasted in each breathing cycle (McCoy 2000). The high cost of packaged gas O_2 and its home delivery coupled with decreasing medical reimbursement payments motivated the development of oxygen conserving devices (OCD) to reduce the

waste and thereby reduce the cost of O_2 used. OCDs were first introduced as intermittent flow devices that limit the continuous flow of O_2 to the patient to only the inspiration period (demand type) or provide a high flow pulse or dose of O_2 during the early part of the inspiration period of each breath cycle. An OCD is typically triggered by the reduction in pressure at the beginning of the inspiration cycle. This signals the opening of a valve to supply O_2 for a given time or fixed dose volume. Increased breathing rate is detected in more sophisticated devices and O_2 supply rate is automatically increased to maintain a fixed pulse volume (and near fixed F_{IO2}). This is in contrast to continuous flow where the F_{IO2} decreases with increased breathing rate (Bliss et al. 1999; Carlin et al. 2018).

McCoy (2000) provided an example of F_{IO2} levels achieved as a function of continuous flow oxygen supply for a fixed set of normal breathing parameters, i.e. breathing rate, tidal volume, dead space volumes, etc. F_{IO2} increased linearly from 24% at a continuous flow of 1.0 lpm to 44% at 6.0 lpm. Because OCDs reduce the amount of O_2 supplied compared to a given continuous flow rate, OCD providers began marketing these devices on the basis of "equivalency" to continuous flow, e.g. OCD settings of 1–5 equivalent to continuous flow of 1–5 lpm, respectively. However, each OCD setting provides a fixed amount of O_2 which may or may not result in the same or "equivalent" F_{IO2} at the so-called corresponding lpm flow rate depending upon the individual patient (Dunne 2009; Chatburn and Williams 2010; Carlin et al. 2018). The F_{IO2} vs. continuous flow characteristic is unique to each patient depending upon the patient's breathing characteristics. Furthermore, O_2 saturation levels may also vary for a given F_{IO2} level depending upon the physiological condition of the patient. The OCD technology is one of the important enablers to the development of POCs. In order to overcome the confusion created by the original "equivalency" concept, it appears that the industry is moving toward verifying patient O_2 saturation levels directly for specific POC devices. Furthermore, physicians are beginning to recognize that a LTOT prescription should be based upon O_2 saturation level rather than an arbitrary lpm flow rate.

The O_2 concentrator market has been growing continuously since the introduction of the stationary O_2 concentrator and is accelerating due to the development of portable concentrators. Jacobs, et al. (2018) suggests that more than 1.5 million adults in the US are using supplemental O_2 for a variety of respiratory disorders. A recent Global Market Insights report (2018) estimated the 2017 world market for O_2 concentrators to be USD 1.3 billion.[1] The market appears to be split about equally between stationary and portable devices.

3.1 Stationary O_2 concentrators

Stationary concentrators are continuous flow devices (Fig. 1) designed for use in the home, operate on alternating current (AC), can be rolled around inside the home but are not easily transportable outside the home. Properly maintained, these devices are well established and have demonstrated reliable performance. They provide an unlimited supply of O_2 as long as electricity is available. The patient is tethered to the device via a long supply tube connecting the concentrator to a nasal cannula, allowing the patient to walk from room to room with the concentrator remaining stationary. The most common units provide up to 5 lpm O_2 at a nominal purity of 90%. A higher rate version (0–10 lpm) is offered for more critical patients who need higher O_2 flow rates. With respect to a physician's prescription for LTOT, stationary concentrators have been a "one size fits all" solution to providing supplemental O_2. The patient's O_2 saturation levels still need to be verified for the prescribed flow [historically 2 lpm (Dunne 2009)], but excess flow capacity is available if increased flow is required. Essentially all of the stationary units provide variable flow rate capability and the same O_2 purity. As a result, there is little uncertainty in the selection of the device and its capability to meet the patient's O_2 requirements.

Table 1 summarizes the basic characteristics of stationary 5 lpm O_2 concentrators extracted from the product literature of six major concentrator manufacturers. The units vary in weight from a low of 18 lb to a high of 54 lb, with a typical weight in the range of 30–36 lb. The power consumption varies from 275 to 385 W at the maximum flow rate of 5 lpm. Noise levels appear to be consistent in the 45–50 dB range and outlet pressure is typically 5 ± 0.5 psig. The outlet pressure listed by the manufacturer reflects the pressure required to overcome the resistance of the supply tubing and nasal cannula, as well as for flow control (Kaplan et al. 1989). This supply pressure is regulated from the higher concentrator O_2 product pressure. Higher O_2 purity levels are achieved when operating the concentrator at the lower flow rates, assuming that the feed pressure and cycle times remain unchanged.

Table 2 summarizes the basic characteristics of stationary concentrators with maximum O_2 product flows of 8–10 lpm extracted from the product literature of five major concentrator manufacturers. Weight, noise and power consumption are higher than the 5 lpm counterparts. Higher outlet pressures varying from 10 to 20 psig are reported.

[1] Information taken from an abbreviated summary of the full report. Full report available at a significant cost.

Table 1 Stationary concentrators (0–5 lpm)

Manufact	Model	O_2 Flow lpm	O_2 purity %	Wt lb (kg)	Power watts	Outlet P_{O2} psig	Noise dBA	Source
Caire, Inc	AirSep VisionAire™ 5	1–5	90 + 5.5/− 3	30 (13.6)	290		45	https://files.caireinc.com/ML-CONC0073.pdf Accessed 13 April 2019
	Caire Companion 5™	0.5–5	90 + 5.5/− 3	36 (16.3)	385 @5lpm	4.6		
	AirSep NewLife® Elite	1–3	95 + 0.5/− 3	54 (24.5)	350	7–9	48	
		4	92 + 3.5/− 3					
		5	90 + 3.5/− 3					
Inogen	At Home GS100	1–5	90 + 6/− 3	18 (8.2)	275 max		< 50	https:/www.inogen.com/pdf/96-05070-00-01c-Technical-Manual-Inogen-AT-Home.pdf Accessed 4 January 2019
Philips Respironics	EverFlo Q	0.5–5	93 ± 3	31 (14.1)	350	5.5	45	https://philipsproductcontent.blob.core.windows.net/assets/20,170,523/83580c74bf0a14da77c015995be.pdf60f8d8 Accessed 4 January 2019
Invacare®	Perfecto2™ V	0.5–5	90 + 5.6/− 3	40 (18.1)	325	5 ± 0.5	≤ 53	www.invacare.com/doc_files/1193322.pdf Accessed 7 January 2019
Drive Medical DeVilbiss Healthcare	Devilbiss 5L Oxygen Conc. 525DS	0.5–5	90 + 6/− 3	36 (16.3)	310	8.5 ± 0.5	48	https://cdn.drivemedical.com/media/files/3061/A-525D3%20Rev%20C.pdf Accessed 8 January 2019
GCE® Healthcare	Nuvo Lite Mark 5	5	90 + 6.5/− 3	32 (14.5)	300		40	https://www.gcehealthcare.com/wp-content/uploads/2018/01/735,100,000,395.pdf Accessed 21 January 2019

Several of the concentrator manufacturers provide prices online for direct purchase by patients. List prices for 5lpm units varied from US$800 to US$1500, while the price of one 10lpm unit was US$2000. Cost of these units when purchased by durable medical equipment providers (DME) may be different. DMEs purchase concentrators from the manufacturer, provide the equipment to the patient and are reimbursed by the health insurance or other agency.

Published studies evaluating the concentrator PSA process and/or adsorbent characteristics are sparse. The product specifications provide some insight into the PSA process, e.g. the product (O_2) purity, outlet pressure and unit weight. It appears that most stationary concentrators are two-bed, PSA units. Reviewing concentrator manuals, parts lists, diagrams and compressor manufacturer specifications leads to the conclusion that the primary contributor to weight and power consumption is the compressor. Such generalizations may not apply to all stationary units, e.g. the lighter weight and lower power consumption of the Inogen At Home GS100 suggests a process with higher O_2 recovery and a correspondingly smaller, more efficient compressor.

3.2 Portable O_2 concentrators

Portable O_2 Concentrators (POC) appeared in the mid-to-late 1990s and their use has increased dramatically over the last decade. This clearly represents a disruptive technology to the concentrator market. Portability has been enabled by a combination of technologies including intermittent flow control, Li-ion batteries, lightweight compressors and vacuum pumps and smaller fast-cycle PSA units. POCs are available from various manufacturers in pulse flow and combined pulse flow/continuous flow modes as illustrated in Fig. 1. The major advantage to the patient is increased mobility (including air travel) and activity resulting in an improved quality of life. Some patients are using a POC for all their LTOT, i.e. inside and outside the home. DMEs are also bundling a POC with a stationary O_2 concentrator to

Table 2 Stationary concentrators (0–8 lpm and 0–10 lpm)

Manufact	Model	O_2 Flow lpm	O_2 purity %	Wt lb (kg)	Power watts	Outlet P_{O2} psig	Noise dBA	Source
Caire, Inc	AirSep NewLife® Intensity	8 10	90 + 5.5/− 3	54 (24.5) 58 (26.3)	410 590	20	52 55	https://files.caireinc.com/ML-CONC0073.pdf Accessed 13 April 2019
Philips Respironics	Millennium M10	1–10	92 ± 4	53 (24)		10–30		https://www.usa.philips.com/healthcare/product/HCM10600/millennium-M10-Oxygen-concentrator-specifications Accessed 7 January 2019
Invacare®	Platinum™ 10L	2–10	90 + 5.6/− 3	53 (24)	585	9 ± 0.5	≤ 62	www.invacare.com/doc_files/1193323.pdf Accessed 8 January 2019
Drive Medical DeVilbiss Healthcare	Devilbiss 10L Oxygen Conc. 1025DS	2–10	90 + 6/− 3	42 (19.1)	639	20 ± 1.0	≤ 69	https://cdn.drivemedical.com/media/files/3888/A-1025%20Rev%20C.pdf Accessed 8 January 2019
GCE® Healthcare	Nuvo 8	0.5–8	90 + 6.5/− 3	< 50.7 (< 23)	400	17.4	< 48	https://www.gcehealthcare.com/wp-content/uploads/2018/01/735100000512.pdf Accessed 21 January 2019

meet all the patient's supplemental O_2 requirements. Some patients are purchasing their own POC outright.

A major benefit of POCs is that they can be certified by the Federal Aviation Administration (FAA) for use on board aircraft (FAA 2016). More than twenty such devices have been approved for use on commercial airlines. Two significant limitations imposed by the FAA include a maximum oxygen pressure of 29.0 psig (43.8 psia) and a maximum Li-ion battery size of 100 Wh. Although there are some exceptions to these rules, concentrator manufacturers typically design their POCs within these limitations. The upper limit on pressure is particularly important in the selection of the compressor.

There are no standard performance specifications for POCs and performance varies widely throughout the many POCs available. Various POCs have been tested to determine maximum F_{IO2} and pulse dose output (McCoy 2013; Carlin et al. 2018). The results revealed maximum F_{IO2} ranging from 27 to 41% and maximum O_2 pulse dose varying from 25 to 92 ml at 20 br/min. Clearly, a given patient's supplemental O_2 requirements may not be met by some or all of these concentrators. As mentioned previously, the proliferation of these devices and their variations in O_2 production has resulted in some confusion amongst patients, DMEs, respiratory therapists and physicians relative to appropriate selection and use (Jacobs et al 2018; McCoy 2013; Dunne 2009). Petty (2000) suggested the following criteria for POCs: weight $\leq$ 10 lb, O_2 concentration $\geq$ 90%, minimum flow of 2 lpm for 4 h. Carlin et al. (2018) echoed the importance of these same criteria, although without quantification. Jacobs et al. (2018) suggested a need for POCs with production capacity > 3 lpm. O_2 production capacity (flow rate) and duration are primarily dependent upon battery power. The battery, adsorbent beds and compressor are the major contributors of weight in the device. The variation in performance amongst POCs is essentially the result of differing compromises made between O_2 production capacity, duration and weight, although technology differences may also be a factor.

3.2.1 Pulse flow

While intermittent flow devices or OCDs were originally developed to conserve oxygen, e.g. Kenyon and Puckhaber (1988), their use in POCs is aimed primarily at conserving battery life. Providing a bolus or pulse dose of O_2, synchronized to the patient's breathing pattern, allows the concentrator to operate at a lower "minute volume," which in turn can be exploited to consume less compressor power via lower compressor speed and/or a smaller compressor. "Minute volume" refers to the total volume of O_2 delivered in intermittent pulses over a one minute time period. Concentrator manufacturers typically provide a table of pulse volume at various breathing rates for each POC setting. The product of the pulse volume (at the maximum POC setting) and the corresponding breathing rate represents the maximum O_2 production capacity of the device, i.e. its maximum minute volume.

POCs are typically classified in one of two categories: minute volume or fixed pulse. A simple way of envisioning the operation of a fixed minute volume device is to

consider the progression of POC settings, e.g. 1–5, as representing incremental increases in the flow output of the concentrator through a corresponding increase in the speed of the compressor. Devices that deliver a fixed minute volume at each POC setting are characterized by a declining pulse volume and F_{IO2} with increased frequency of breathing (Chatburn and Williams 2010). Fixed pulse devices deliver a constant pulse volume and F_{IO2} independent of breathing rate, i.e. each setting on the POC represents a different pulse volume. However, the POC is still limited by the maximum production capacity of the PSA system. When this limit in PSA production capacity is reached at high breathing rate, the mode of operation changes to fixed minute volume and the pulse volume will necessarily decrease with increased breathing frequency. In some devices a warning is provided to the user of this condition.

The volume and delivery of the pulse depend upon the triggering sensitivity and the following pulse characteristics: delay time, rise time, peak height and duration. The pulse is triggered at the beginning of inspiration due to a drop in pressure. If the sensitivity (cm H_2O) is too low then a pulse may be missed, while if too high the pulse may be triggered out of sync with the breathing pattern. This parameter is particularly important for patients with dyspnea or shallow breathing (e.g. during sleeping). Outlet pressure varies with pulse setting. Pulse delivery variables have been measured for several POC devices (Chatburn and Williams 2010, 2013).

It should be noted that the PSA air separation unit is a continuous flow process for both types of POC concentrators, producing O_2 and supplying it to a product tank at the design pressure of the process, although there can be a different peak pressure for each pulse setting. The production capacity is thus limited by the design and performance of the PSA unit and the characteristics of the compression equipment. Both fixed minute volume and fixed pulse POCs are pulse-flow only devices. All of the current pulse flow only POCs reviewed here have an O_2 production capacity $\leq$ 1.26 lpm and are not designed to provide supplemental O_2 in a continuous flow mode.

The performance specifications of thirteen pulse flow POCs offered by eight manufacturers are summarized in Table 3.[2] Nine of these devices have a maximum production capacity (maximum O_2 flow rate) or minute volume varying from 0.78 to 1.26 lpm, weigh between 4.8 and 6.8 lb and produce pulse volumes at maximum POC setting ranging from 40 to 63 ml O_2. One parameter for comparing these devices is the specific weight (lb/lpm) or total device weight/O_2 production capacity ratio. It is apparent that there is more than a factor of two difference in this parameter amongst the devices in Table 3. Minimum lb/lpm and maximum duration in combination with a competitive cost is the optimum design target for these devices. A direct comparison of battery duration amongst the devices is difficult because duration is not reported on a consistent basis. Nevertheless, durations are given in the table at setting 2 and 20 br/min. The sources of information in Table 3 are given in Table 4. The remaining four units have limited production capacity (0.52–0.68 lpm) and O_2 pulse volume capability (26–34 ml) at their maximum setting and 20 br/min. Some of these lower flow/lower pulse volume devices provide a lower weight option for patients that require only modest supplemental O_2.

Many of the devices in Table 3 have been evaluated to determine their mode of O_2 delivery, as well as their pulse volume and minute volume characteristics as a function of breathing frequency (McCoy and Diesem 2018; Chatburn and Williams 2010, 2013; Zhou and Chatburn 2014). Such tests were performed using a lung or breathing simulator with the objective to determine performance at the various settings of the devices as it relates to the POC's ability to provide effective supplemental O_2 in LTOT. While these results reflect the production capacity of the PSA unit, the bulk of the data reflect the performance of the POC's intermittent flow component. Most of the devices in Table 3 fall into the "fixed minute volume" category, and performance (F_{IO2}) at any given setting varies considerably from device to device. It is this variability that contributes to a greater difficulty in selecting the most appropriate device for a specific patient. The Zen-O-Lite™ (GCE®) provides a fixed pulse (and constant F_{IO2}) over the largest range of pulse settings and breathing rates amongst the units in Table 3 (McCoy and Diesem 2018), while the Oxlife Freedom (O_2 Concepts) and the SimplyGo Mini (Philips Respironics) provide a fixed pulse for all settings up to 20 br/min and reduce to fixed minute volume operation for higher breathing rates based upon the pulse volume/breathing rate charts provided by the manufacturers. The Easy Pulse devices (Precision Medical) are advertised as vacuum pressure swing adsorption (VPSA) concentrators. While there may be other units in Table 3 that utilize VPSA, most are believed to incorporate PSA process technology.

While none of the devices in Table 3 meet the Petty (2000) requirement noted above, there is a growing belief amongst concentrator manufacturers that pulse flow devices having a production capacity of 1.0 lpm can provide the same level of O_2 saturation in patients as a continuous flow device operating at 5.0 lpm. Such a relationship requires further verification through measurement of the O_2

[2] The information in this table was extracted from the manufacturer's specification sheets, brochures and manuals provided on their respective websites. Device weights and durations generally reflect the basic unit with a single battery installed.

Table 3 Portable O_2 concentrators (pulse flow)

Manufact	Model	Wt lb (kg)	O_2 purity %	PF (setting)	Max O_2 Flow lpm	Pulse ml @ 20br/ min	Battery duration h	Mass/ Unit O_2 Flow[a] lb/lpm
Caire, Inc	FreeStyle™ 3	4.4 (2)	90 + 5.5/− 3	PF (1–3)	≈ 0.52	26.0 Setting 3	2 @ Setting 3	8.5
	FreeStyle™ 5	6.2 (2.8)	90 + 5.5/− 3	PF (1–5)	≈ 0.97	48.4 Setting 5	1 @ Setting 5	6.4
Inogen	Inogen One® G4	2.8 (1.3)	90 + 6/− 3	PF (1–3)	0.63	31.5 Setting 3	2.7	4.4
	Inogen One® G3	4.8 (2.2)	90 + 6/− 3	PF (1–5)	1.05	52.5 Setting 5	4.7	4.6
	Inogen One® G5	4.8 (2.2)	90 + 6/− 3	PF (1–6)	1.26	63.0 Setting 6	4.5	3.8
Philips Respironics	SimplyGo Mini	5 (2.3)	90 + 6/− 3	PF (1–5)	1.00	50.0 Setting 5	4.5 @ Setting 2	5.0
Invacare®	Platinum™ Mobile	4.9 (2.2)	90 + 5.6/− 3	PF (1–4)	0.88	44.0 Setting 4	3.5 @ Setting 2	5.6
	XPO_2™	6.4 (2.9)	90 + 5.6/− 3	PF (1–5)	0.84	42.0 Setting 5	2.4 @ Setting 2	7.6
ResMed	Mobi™	5.5 (2.5)	90 + 6/− 3	PF (1–4)	0.68	34.0 Setting 4	6.0 @ Setting 2	8.1
O_2 Concepts	Oxlife Freedom	5.9 (2.7)	91 ± 4	PF (1–5)	0.80	40.0 Setting 5	3.5 @ Setting 2	7.4
GCE® Healthcare	Zen-O Lite™ RS-00600	5.5 (2.5)	90 + 6/− 3	PF (1–5)	1.05	52.5 Setting 5	4.0 @ Setting 2	5.8
Precision Medical	Easy Pulse PM4130	4.9 (2.2)	90 + 5/− 3	PF (1–3)	0.52	26.0 Setting 3	4.0 @ Setting 2	9.4
	Easy Pulse PM4150	6.8 (3.1)	90 + 5/− 3	PF (1–5)	0.78	39.0 Setting 5	3.2 @ Setting 2	8.7

[a]Calculated from column 3 (Wt) and column 6 (Max O_2 Flow)

saturation levels of patients using a specific device operating at a prescribed setting. Certainly these devices are the most desired by patients due to the low weight and maximum mobility. These factors may explain an increasing concentration in the market toward pulse flow devices of the type in Table 3. Continuing to increase the production capacity and/or duration of these POCs (within current or decreasing device weight) presents challenges in compressor, battery and adsorption technologies.

PSA performance has been reported for the Invacare® XPO_2™ listed in Table 3 (Rama Rao et al. 2014d). The two bed unit produced 0.7–0.9 lpm 90% O_2 using a cycle that varied from 10 to 14 s. BSF (200–271 lb/TPDO) and O_2 recovery (23–29%) were determined from the evaluation. No details were provided on how the measurements were made. The results suggest approximately 0.4 lb adsorbent in this device (≈ 0.53 lb/lpm). It is interesting to note that this adsorbent lb/lpm represents a relatively small portion of the overall device lb/lpm.

The manufacturers of these devices offer a wide range of accessories, including AC/DC power options, additional batteries, carrying cases, etc. While many of these accessories are designed to provide additional convenience and extend life, they also add to the overall weight. Most

Table 4 Source information for pulse flow POCs (Table 3)

Manufact	Model	Source
Caire, Inc	FreeStyle™ 3	https://files.caireinc.com/POC-combo-US-ML-CONC0071_A-4b.pdf
	FreeStyle™ 5	https://files.caireinc.com/Titration-Chart-ML-CONC0075_A-2b.pdf
		Accessed 15 April 2019
Inogen	Inogen One® G4	https://www.inogen.com/pdf/InogenOneG4TechnicalManual.pdf
		https://www.inogen.com/MKT02201PulseDoseEfficiencyBrochureWeb.pdf
		Accessed 4 January 2019
	Inogen One® G3	https://www.inogen.com/pdf/96-03996-00-01-RevF_Technical-Manual_Inogen-One-63.pdf
		https://www.inogen.comMKT-0290F-DTP-G3-Single-Sheet.pdf
		Accessed 4 January 2019
	Inogen One® G5	https://www.inogen.com/pdf/96–08,649-00–01 B_G5_English_UserManual-web.pdf
		Accessed April 4 2019
Philips Respironics	SimplyGo Mini	https://philipsproductcontent.blob.core.windows.net/assets/20170523/1560d7ece4ed4cdcb212a77c016692a3pdf. Accessed 7 January 2019
Invacare®	Platinum™ Mobile	www.invacare.com/doc_files/1194969.pdf
		Access 7 January 2019
	XPO_2™	www.invacare.com/doc_files/1148112.pdf
		Access 7 January 2019
ResMed	Mobi™	https://www.resmed.com/us/dam/documents/products/oxygen/Mobi/providers-guide/mobi_providers-guide_amer_eng.pdf
		Access 8 January 2019
O_2 Concepts	Oxlife Freedom	https://o2-concepts.com/wp-content/uploads/2018/10/800-1049_Oxlife_ Freedom_ User_Manual_9-19-18.pdf
		Accessed 9 January 2019
GCE® Healthcare	Zen-O Lite™ RS-00600	https://www.gcehealthcare.com/wp-content/uploads/2017/10/Zen-O-lite_user_manual_en_de_fr_nl_es_pt_it_sv.pdf
		https://www.gcehealthcare.com/wp-content/uploads /2018/10/DL-00497_ZenOlite_leaflet _GCE.pdf
		Accessed 15 December 2018
Precision Medical	Easy Pulse PM4130	https://www.precisionmedical.com/files/literature/506640rev-17.pdf
		Accessed April 8 2019
	Easy Pulse PM4150	https://www.precisionmedical.com/files/literature/507719-pm4150-service-manual-rev-2.pdf
		Accessed April 8 2019

manufacturers recommend servicing (if required) by an authorized service center, although Inogen and GCE® provide replacement sieve beds for installation by the patient. Depending upon the manufacturer's specifications, sieve bed life varies between 12 and 24 months. Online listed prices for some of these devices range from US$2500 to US$3500, excluding accessories. The replacement sieve beds (where offered) range in price from about US$100 to US$150 for a pair of beds, indicating that the cost of the adsorbent and beds are relatively minor component costs in the system. The compressor and battery represent more significant costs to the system.

3.2.2 Combination pulse flow/continuous flow

The desire for continuous flow in a portable device reflects the concern for patients with greater O_2 requirements, shallow breathing characteristics and use during sleep (Chatburn et al. 2006). The trend toward using a POC for all of the patients LTOT increases these concerns. Several concentrator manufacturers also offer a combination pulse flow/continuous flow device, i.e. with two distinct modes. The specifications for six such devices are summarized in Table 5. These POCs range in weight from 10 to 20 lb and are typically transported by the patient using a two-wheeled cart with handle similar to a small suitcase. This is in contrast to the lighter weight pulse flow only devices where patients usually carry the device using a shoulder strap.

Table 5 Portable concentrators (combination pulse flow/continuous flow)

Manufact	Model	Wt lb (kg)	O_2 purity (%)	CF (lpm) or PF (setting)	Max O_2 Flow lpm	Pulse ml	Battery duration (h)	Source
Caire, Inc	Eclipse 5™	18.4 (8.4)	90 + 5.5/− 3	CF (0.5–3.0)	3.0		2.0 @ 2lpm	https://files.caireinc.com /POC-combo-US-ML-CONC0071_A-4b.pdf /Titration-Chart-ML-CONC0075_A-2b.pdf Accessed 15 April 2019
				PF (1–9)	3.0	102 @ 20br/min Setting 6	5.1 @ Setting 2	
Philips Respironics	SimplyGo	10 (4.5)	90 + 6/− 3	CF (0.5–2.0)	2.0		0.9 @ 2lpm	https://philipsproductcontent.blob.core.windows.net/assets/20170523/8d155caa58f849df0a77c0166c013.pdf Accessed 7 January 2019
				PF (1–6)	2.0	72 @ 20br/min Setting 6	3.0 @ Setting 2	
Drive Medical DeVilbiss Healthcare	iGo®	19 (8.6)	91 ± 3	CF (1–3.0)	3.0		2.4 @ 2lpm	https://cdn.drivemedical.com/media/files/3079/A-306-1%20Rev%20H.pdf Accessed 8 January 2019
				PF (1–6)	3.0	NA	4.7 @ Setting 2	
O_2 Concepts	Oxlife Independence	20.3 (9.2)	91 ± 4	CF (0.5–3.0)	3.0		1.25 @ 2lpm	https://o2-concepts.com/wp-content/uploads/2018/05/ Independence-User-Manual-DNA-800–1029-Rev-B.pdf Accessed 9 January 2019
				PF (0.5–6)	3.0	96 @ 20br/min Setting 6	2.9 @ Setting 2	
GCE® Healthcare	Zen-O™ Model RS-00500	10.3 (4.7)	90 + 6/− 3	CF (0.5–2.0)	2.0		0.75 @ 2lpm	https://www.gcehealthcare.com /wp-content/uploads/2018/01 /zeno _leaflet_00477_ZenO_180,112.pdf /wp-content/ uploads/2017/08/ Zen-O_user_manual_en_de_frnl_es_pt_it_sv.pdf Accessed 21 January 2019
				PF (1–6)	2.0	66 @ 20br/min Setting 6	4 @ Setting 2	
Precision Medical	Easy Pulse PM4400	11.4 (5.2)	90 + 5/− 3	CF (0.25–2.0)	2.0		0.80 @ 2 lpm	www.precisionmedical.com/files/literature/508217rev3.pdf Accessed April 8 2019
				PF (1–5)	0.78	39.0 Setting 5	3.0 @ Setting 2	

The maximum O_2 output of these devices is either 2.0 lpm or 3.0 lpm, regardless of the flow mode. The maximum O_2 pulse dose ranges from 66 to 102 ml at the maximum setting and 20br/min, i.e. in most cases nearly twice the pulse volume (and minute volume) provided by the smaller pulse flow only devices of Table 3. In continuous flow mode, these devices are generally limited to approximately 1–2 h at the maximum flow setting. Comparison of duration in pulse flow mode is again difficult due to an inconsistent set of characteristics. Duration in pulse flow mode varies at a setting of 2 from about 3 to 5 h. The higher O_2 production capacity of these devices clearly necessitates a larger compressor and battery or the use of multiple batteries, all of which contribute to increased weight and restricted mobility. The higher production capacity supports fixed pulse operation, e.g. Eclipse 5™ (Caire Inc.) and Zen-O™ (GCE®). Dual mode units (similar to those in Table 5) have been evaluated in use by

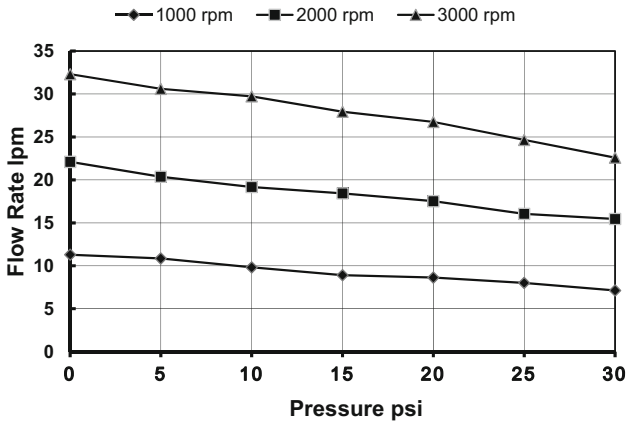

Fig. 2 Pressure/flow characteristics for Gardner Denver Thomas Piston Pump (Model 2220Z)

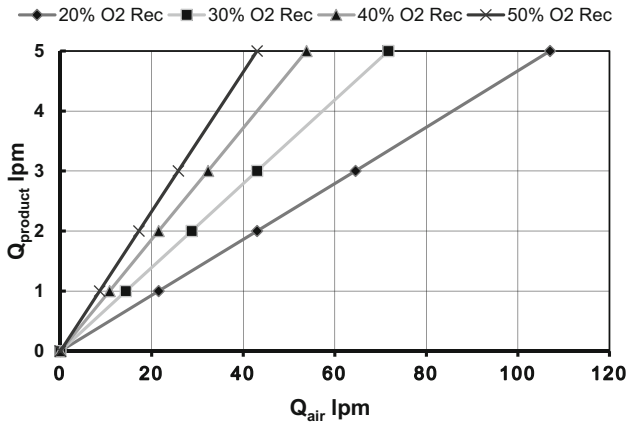

Fig. 3 Variation in required air flow as a function of O_2 production capacity and O_2 recovery

patients during exercise (LeBlanc et al. 2013). The design of these devices appear to be directed at meeting the Petty (2000) criteria, although the combination of weight and duration remain significant challenges.

3.2.3 Compressors/pumps

The mechanical compressor and/or vacuum pump are essential components in the concentrator. According to Chatburn and Williams (2013), "the compressor typically consumes greater than 80% of the power of the system and generates the majority of the noise and all of the vibration of the system." Scroll type compressors (standard and custom designed) for O_2 concentrators can be obtained from Air Squared, Inc. (2019). Another major manufacturer of small compressors/pumps is Gardner Denver Thomas, Inc. (2019a). The website shows at least thirteen different models of compressors/vacuum pumps for potential application in O_2 concentrators.[3] This equipment utilizes a unique patented WOB-L® piston technology.

Several of these units have characteristics consistent with those used in stationary O_2 concentrators, e.g. weight, maximum flow and maximum pressure ratings ranging from 12–18 lb, 65–130 lpm and 40–100 psig, respectively. These units are characterized by AC input power with power consumption consistent with that for the concentrators listed in Tables 1 and 2. Configurations include pressure or vacuum and simultaneous pressure/vacuum parallel flow. Two additional models (2450Z and 2320Z) offer lower weight ($\approx$ 7 lb), high flow ($\approx$ 100 lpm) and intermediate pressure (35–60 psig) options.

Units designated for potential use in "portable oxygen concentrator" operate with either 12 V DC or 24 V DC and have variable output speed from 1000 to 3000 rpm. All of these units have a maximum output pressure of 30 psig. Some compressors are configured for pressure only, while others can be used in either pressure or vacuum mode. A dual head unit, Model 2250Z (Gardner Denver Thomas 2019b), uses a single motor to drive both vacuum and pressure heads simultaneously. The weights of these compressors vary from 0.85 lb to 2.8 lb, while maximum flow (free flow at zero back pressure) ranges from 13.5 to 54.4 lpm. A typical flow/pressure characteristic for this type of machine is illustrated in Fig. 2 for Model 2220Z (Gardner Denver Thomas 2019c). Flow decreases with increasing pressure, a characteristic that is important in the design of the PSA process. All of these units require a motor controller and supplemental cooling air provided by the customer. It is presumed that POC settings represent various controlled motor speeds which correspond to specific minute volume production capacity and power consumption. Some POC manufacturers are known to use Gardner Denver Thomas compressors/pumps, while others design their own compressors, e.g. McCombs et al. 2009.

Although the O_2 production capacity of the concentrators vary from less than 1.0 lpm to as much as 10.0 lpm, the actual air flow processed by the compressor is much larger because 78% of the air is N_2. The actual compressor flow required for a given O_2 production capacity depends heavily upon the O_2 recovery of the PSA process. Figure 3 demonstrates how the required air flow through the compressor varies for a desired O_2 production capacity of the POC as a function of the O_2 recovery of the process (assuming continuous operation of the compressor over the entire PSA cycle). O_2 recovery is defined by Eq. 1.

$$O_2\,Recovery = \frac{(y_{O_2} \times Q)_{product}}{(y_{O_2} \times Q)_{air}} \quad (1)$$

[3] Gardner Denver Thomas compressors are included here as a matter of convenience to represent compressor characteristics in later discussion of the important design factors in the PSA process.

The O_2 product purity is 0.9 (90%) and the O_2 concentration in air is 0.2095 for this example. Clearly the O_2 recovery has a major impact upon the size of compressor required and the corresponding energy consumption. Conversely, higher O_2 recovery provides an increase in production capacity for a given compressor (air flow).

One of the smaller compressors that can produce a useful flow at a useful pressure for POCs is the Model 230Z (Gardner Denver Thomas 2019c). The power consumed by this 1.2 lb compressor at a rated pressure of 30 psig is 34.3 W, 44.7 W and 65.8 W for motor speeds of 1000 rpm, 2000 rpm and 3000 rpm, respectively. Using Chatburn and Williams (2013) approximation of 80% of the total power is attributed to the compressor, it is estimated that the maximum power at the highest rpm (and highest pulse setting) for this compressor would be 82.3 W. Considering the FAA limitation on battery size to be 100 Wh, a POC with this compressor would have a duration of about 1.5 h at its maximum pulse setting and 30 psig (corresponding to a maximum air flow of 11.3 lpm). An O_2 recovery of about 38% would be required for an O_2 production capacity of 1.0 lpm. Operating at lower motor speeds (rpm), lower peak pressure and lower flows would result in lower power and longer durations – perhaps as much as 3.0–4.0 h for this compressor. Such durations are reasonably consistent with those reported for the POCs in Table 3. The power estimated for intensified MOC cycles operating with a continuous O_2 flow and high rate LiX adsorbents varied from 33.9 to 56.5 W/lpm (15–25 kW/TPDO) (Ackley and Zhong 2003d).

3.2.4 Batteries

The battery technology is an important component with respect to POC portability (size and weight), O_2 production capacity (compressor size and power) and duration. Any increase in battery energy per unit mass would be a direct benefit to POC operating duration. The availability of AC and DC power options, spare batteries and battery chargers relieves somewhat the demand on longer operation on a single battery. Although cost effective improvements in battery technology would undoubtedly be captured in POC products, considerations of such prospects is beyond the scope of this review. Several suppliers of Li-ion batteries have been identified by Bliss et al. (2010).

4 Progress in air separation technology

Air separation to produce 90% O_2 product is perhaps the most demanding of bulk gas separations by adsorption, i.e. simply because the heavy component (N_2) accounts for $\approx$ 78% of the feed air. Numerous elements must be integrated to accomplish this separation, e.g. an N_2-selective adsorbent with high N_2 working capacity and N_2/O_2 working selectivity, a pretreatment layer to remove H_2O and CO_2 and a pressure swing cycle tailored to the characteristics of the adsorbent within the constraints of available compression equipment. Adsorption and desorption within the bed are affected by multi-component thermodynamics, temperature gradients, heat and mass transfer, air flow velocity and the physical properties of the adsorbent particles. Separation performance may depend upon the number of beds, system void volumes and pressure drop. Dense packing of the beds and fluidization can be important factors in achieving optimum O_2 production. Taken individually, many of these elements may seem to be conceptually straight forward. However, integrating all of them to achieve a high performance process with respect to high O_2 purity, low bed size factor (BSF), low power and high O_2 productivity at a competitive cost is not trivial.

A principal aim of this review is to highlight some of the most important developments in adsorptive air separation, particularly those related to the elements listed above. Many of the published studies were driven by industrial air separation, but also apply to the progress made in MOCs. According to Chai et al. (2011), 452 US Patents were issued between 1980 and 2005 on adsorptive air separation. Indeed, much of the reported research impacts adsorption processes beyond air separation. The various elements can generally be categorized within either adsorbent research or process development, although ultimately it is the overlapping and cooperative efforts of these two disciplines that have achieved the greatest success. With respect to process development, intensification has been particularly important in applying industrial air separation technology at the scale of MOCs.

4.1 Adsorbents

The introduction of synthetic crystalline aluminosilicates (zeolite molecular sieves) enabled the commercialization of numerous gas separations. The framework of these microporous materials consists of primary tetrahedra (SiO_4 and AlO_4) and secondary building units (Breck 1974). The inherent charge neutrality of the structure requires the introduction of charge balancing cations to offset the charge deficit created by the Al^{3+} in the structure. The presence of these cations creates non-uniform electrostatic fields within the zeolite cavity that are largely responsible for adsorption of gas molecules. Molecules entering the zeolite cavity are adsorbed to varying degrees depending upon the interaction between the electrostatic fields of both the adsorbate molecules and those internal to the structure (Ruthven 1984). The Si/Al ratio, cation type(s), cation size

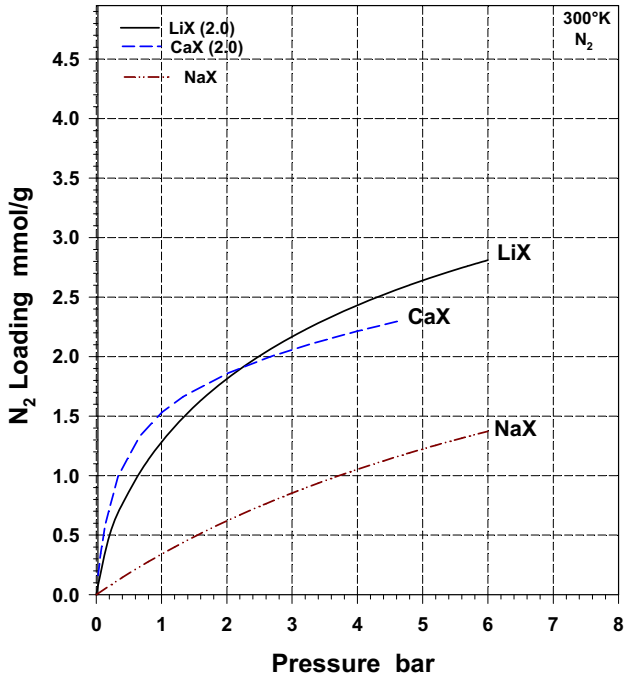

Fig. 4 N_2 isotherms for LiX, CaX and NaX

and location all affect these internal electrostatic fields. Gas molecules are adsorbed in the micropore volume defined by the cavities within the ionic structure. Adsorption in zeolites is often referred to as "pore filling"—in contrast to surface adsorption or specific site adsorption. Type X zeolite is a particularly good pore filling adsorbent because of its large cavities and pore volume.

4.1.1 N_2 selective zeolites

The preferential selectivity of N_2 over O_2 in zeolites with lower Si/Al is attributed to the different quadrupole moments of N_2 and O_2 and their respective interactions with the non-uniform electrostatic fields within the zeolite structure (Breck 1974; Yang 2003). Such selectivity is considered "equilibrium selectivity" in that the adsorption capacity of N_2 is much greater than that of O_2 as revealed in the pure component equilibrium isotherms of the two gas species. Types 5A (CaA) and 13X (NaX) were the first widely used zeolites for air separation. However, other zeolite frameworks and cation compositions also have N_2-selective characteristics. Coe and Kuznicki (1984) patented several polyvalent ion exchanged type X zeolites for air separation with particular emphasis upon the proper thermal activation methodology. Kuznicki et al. (1986) synthesized "maximum aluminum" type X zeolites with Si/Al = 1.0. Within the Type X and Type A frameworks alone, there are many possible N_2-selective adsorbents resulting from single cations and mixed cation

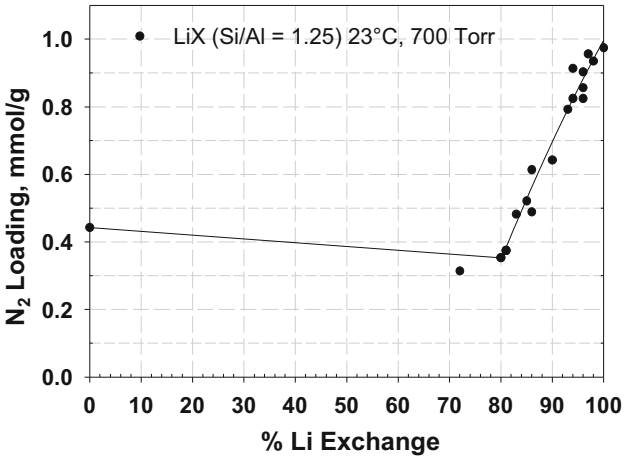

Fig. 5 N_2 loading at various Li exchange %

compositions. Such compositional variations in the zeolites produce a wide range of N_2 capacity and isotherm shapes as illustrated by the example of LiX, CaX and NaX isotherms shown in Fig. 4. With the exception of a few Ag-exchanged zeolites, there is little to no Ar/O_2 selectivity in these types of zeolites (Knaebel and Kandybin 1993; Yang 2003; Wu et al. 2015). As a result, Ar remains in the same proportion to O_2 as it is in the feed air in both the adsorbate and in the product. This characteristic limits the maximum O_2 product purity to $\approx$ 95.7% with complete removal of N_2 from air. Two good reviews of progress in the development of air separation adsorbents are provided by Gaffney (1996) and Yang (2003).

The most important adsorbent discovery affecting present day air separation processes for O_2 production is that of Chao (1989) for LiLSX, i.e. high Li-exchange type X with Si/Al = 1.0 (also known as low silica X or LSX). A unique property of LiX is the progressive filling of cation sites wherein the first $\sim$ 67–80% of Li exchange results in cations residing in sites with little exposure to the adsorption space (increased filling beginning at lower Li exchange levels for lower Si/Al). As a result, the interactions between Li^+ and N_2 gas molecules are weak. The remaining exchange of Li^+ up to 100% results in a dramatic and linear increase in N_2 adsorption capacity as illustrated for LiX (Si/Al = 1.25) (Chao 1989) in Fig. 5 (Ackley 2003a). In this figure, 0%Li corresponds to 100%Na. When the Si/Al ratio is reduced from 1.25 to 1.0, the number of monovalent cations required to balance the structure charge increases from 86 to 96, respectively. This results in additional N_2 capacity as well as reduced O_2 capacity, thereby increasing N_2/O_2 selectivity.

Soon after Chao's invention, processes were developed to exploit the superior air separation adsorption characteristics of LiX. As processes improved, greater demands were imposed upon adsorbent performance. Advances in

LiX technology have been continuing over several decades through improved binders and reduced binder content, improved adsorption rate and increased level of Li exchange. This has necessitated improvements in LiX manufacturing methods with regard to efficient Li exchange, activation, smaller beads and adsorbent yield. Some examples of these developments include the following: conversion of clay binder to zeolite by caustic digestion to improve both N_2 capacity and rate (Plee 2001; Chao and Pontonio 2002; Plee 2003); fibrous and hollow tube clay binders aimed at reducing binder content and improving rate (Hirano et al. 2001; Weston et al. 2007; Weston et al. 2018); silicone-derived binding agents for improved pore structure, N_2 capacity and rate (Barrett et al. 2015); and innovative Li recovery methods (Leavitt 1995, 1997). Additional N_2 and O_2 isotherms for a variety of LiX compositions representing different binders, binder content and Li exchange levels can be found in the literature, e.g. Baksh et al. 1992; Park et al. 2014; Zheng et al. 2014, Wu et al. 2014a, b.

A common problem encountered with all new zeolite compositions is the economic manufacturing of these materials. High yield, consistent bead size, porosity and strength, high cation exchange, low water content and thermal stability while maintaining the desired adsorption characteristics are some of the important concerns that must be addressed (Zheng et al. 2014). The rising cost of LiCl due to increased demand for manufacturing Li-ion batteries has also affected LiX economics. Full scale manufacturing methods and equipment often cannot be represented in the laboratory. Thus, successful scale-up of zeolite manufacturing processes is often uncertain.

There has always been a compromise between adsorbent bead strength and transport resistance, i.e. an apparent inverse relationship between density and porosity. However, porosity as conventionally determined by Hg porosimetry does not consistently correlate to adsorption rate (Ackley and Leavitt 2002; Ackley et al. 2017). Such methods are insufficient in describing the complex morphology of the macropore structure that determines the intrinsic diffusivity of the adsorbent. The macropore morphology of the agglomerated zeolite and the resultant bead strength are largely dependent upon the physical properties and relative amounts of the zeolite powder and binder, as well as the agglomeration method. A new model-based approach aims to create adsorbents with improved pore structure and strength while maintaining or increasing N_2 adsorption rate and N_2/O_2 selectivity. Three dimensional (3D) representations of the pore structure are stochastically reconstructed from 2D digitized images of scanning electron micrograph (SEM) cross-sections of existing adsorbents (Kikkinides and Politis 2014a). These 3D adsorbent representations are then used to simulate diffusion of N_2 probe molecules in the void space (Kikkinides and Politis 2014b). Hypothetical adsorbent models are then developed by combining zeolite crystallite and binder spherical particles in various packing arrangements to study pore diffusivity in the engineered pore structures. Application of these methods has resulted in a prescription for high rate adsorbent compositions that include specifications for the mean diameters of the adsorbent powder and binder particles, binder concentration and median pore diameter (Ackley et al. 2017). Following this recipe leads to a preferred combination of particle porosity and intrinsic N_2 pore diffusivity.

4.1.2 Pretreatment layer—removal of H_2O and CO_2 from air

N_2-selective zeolites are also excellent adsorbers of the polar molecules H_2O and CO_2 typically present in air. While CO_2 and N_2 may be co-adsorbed, H_2O is preferentially adsorbed to the exclusion of N_2 and other gas molecules (Peterson 1981), thereby rendering the N_2-selective adsorbent ineffective for air separation. As little as 2.0wt% water adsorbed can result in more than 50% reduction in N_2 capacity. To avoid this situation a pretreatment layer (e.g. comprising NaX zeolite, activated alumina or silica gel) is added to remove H_2O and CO_2 from air prior to the air entering the active N_2-selective adsorbent layer (Yang 1987). Even when there is no pre-layer ahead of the main N_2-selective adsorbent, "water adsorption creates a de facto inert layer" that acts in a similar manner as a pretreatment layer (Wilson et al. 2001). While water vapor is more easily desorbed by alumina in a PSA process, lower dew point is achieved with a zeolite NaX. The significance of this difference in adsorbent characteristics is that insufficient removal of H_2O can lead to a slow contamination of the N_2-selective layer known as "water creep." An H_2O concentration of only 1.0 ppm in equilibrium with X-type zeolites corresponds to more than 2.0 wt% H_2O loading. Water contamination is the chief reason for ending the life of the N_2-selective zeolite, although it is possible to restore the adsorbent to its initial condition by removing and regenerating it.

The penetration of water in the pre-layer was estimated by modeling under vacuum swing adsorption (VSA) conditions (Wilson et al. 2001). A depth of 300 mm for a NaX pre-layer was suggested as typical for industrial air separation. It was also suggested that the N_2 adsorption capacity of the main adsorbent layer would be significantly inhibited by H_2O adsorption levels as low as 1.0 wt%.

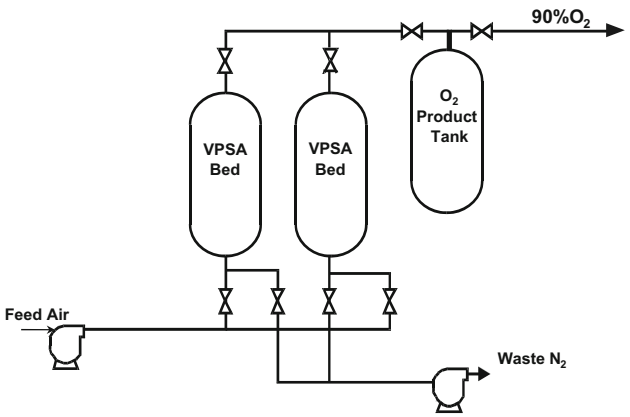

Fig. 6 VPSA system for air separation

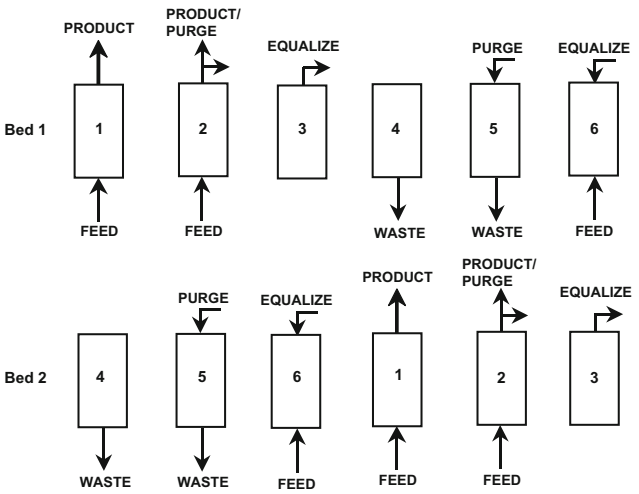

Fig. 7 Six step cycle diagram

4.2 Cyclic adsorption processes

Following the inventions of Skarstrom (1960, 1966) and Guerin De Montgareuil and Domine (1964), numerous processes for separating air by PSA for O_2 production were developed. Some notable process inventions include the following: pressure equalization and/or product purge (Berlin 1966); VSA cycle utilizing a variety of cation exchanged Type X and Type A zeolites (Berlin 1967); three-bed PSA with the introduction of simultaneous product and feed pressurization cycle steps using CaA zeolite (Batta 1972); increasing pressure adsorption feed step (McCombs 1973); three-bed VPSA cycle with countercurrent blowdown to atmospheric pressure using CaA zeolite (Armond and Webber 1975); utilization of waste heat from the vacuum pump to heat feed air (Reiss 1986); low pressure ratio cycles (Leavitt 1991; Smolarek et al. 2000); PSA and VPSA single bed cycles (LaSala and Schaub 1994); overlapping equalization and evacuation steps followed by simultaneous feed and product pressurization (Baksh et al. 1996). The above list represents a cross section of the earlier historical PSA, VSA and VPSA processes developed for air separation for O_2 production. Clearly there are many more patents describing various process strategies to improve performance. Early developments are also described in literature reviews (Cassidy and Holmes 1984; Reiss 1994; Kumar 1996) and in textbooks (Ruthven 1984; Yang 1987; Ruthven, et al. 1994).

Adsorptive air separation is a regenerative (cyclic) process wherein air is introduced to the feed end of the adsorbent bed and N_2 is adsorbed while high purity O_2 is withdrawn from the product end of the bed. The air feed must be terminated prior to the breakthrough of N_2 at the product end of the bed and N_2 saturation of the adsorbent. The adsorbent must then be regenerated to desorb N_2 and prepare the bed for the next cycle. A schematic of a simple two-bed air separation system is shown in Fig. 6. This system shows both a compressor and a vacuum pump applicable to a VPSA process. It becomes a PSA system by simply removing the vacuum pump, and a VSA system by replacing the compressor with a simple fan (an air mover of some sort is required for the feed step in a VSA system). If this were an industrial scale system, then a product compressor could be added to increase the O_2 pressure to meet customer requirements. The choice of process type is largely dependent upon the shape of the N_2 isotherm (see Fig. 4), i.e. the near-linear NaX isotherm favors PSA, the steep portion of the CaX isotherm below 1 atm suggests VSA and the intermediate curvature of the LiX isotherm is best suited to VPSA.

A simple six-step cycle that could be utilized with the system shown in Fig. 6 is illustrated in Fig. 7. The steps shown in this cycle are described as follows: step1 (feed air at pressure and make product); step 2 (continue air feed, make product and use some product for purging other bed); step 3 (equalize down in pressure via bed-to-bed interaction); step 4 (depressurize (blowdown) to atmospheric pressure); step 5 (continue depressurization by evacuation and provide product purge); step 6 (equalize up in pressure, overlapping with feed air pressurization). The steps in the cycle for Bed 1 must synchronize with those in Bed 2, e.g. steps 1, 4, steps 2, 5 and steps 3, 6 must have the same step time as one bed is producing O_2 and the other is being regenerated. One objective is to maintain continuous operation of the compression equipment as shown for the compressor in Fig. 7, i.e. feed in steps 1, 2 and 6. A vacuum pump (if used) would be idle for steps 3 and 6. The purpose of the feed and evacuation steps is obvious, while equalization and product purge steps conserve energy and control the position of the concentration fronts. Introducing O_2-rich gas at the product end of the bed ensures that high

O_2 purity is available at the top of the bed as soon as the make product step begins. As many as twelve or more steps (usually combinations or overlapping of those shown, as well as product pressurization) are possible to improve process performance, e.g. Smolarek et al. (2000). Overlapping of steps, i.e. simultaneously adding or withdrawing gas from both ends of the bed, assists in lower energy consumption and purity control. More beds facilitate such bed interactions, but at the penalty of greater capital cost. Industrial air separation is driven by the cost of O_2, with capital and power costs being the primary contributors. The majority of commercial industrial air separation installations are two-bed systems, consistent with the system optimization strategies of Campbell et al. (1993).

Most of the process and adsorbent developments prior to 1990 were accomplished through small scale laboratory experiments with process scaling factors as great as 1000. Furthermore, there was often a noticeable disconnect between independent process and adsorbent studies. The environment changed as a result of the fortuitous intersection of the following: emergence of a market for 90% O_2 to replace air in several different industrial processes creating both cost and environmental benefits; the discovery of high capacity LiX (Chao 1989) and the improvement in numerical methods coupled with increased computational power. The latter resulted in tools to model and simulate air separation processes – providing an avenue for investigation and a better understanding of phenomena that could not easily be studied by experimentation, e.g. thermal and pressure gradients in the bed, refrigeration effects, working capacity and selectivity, etc. The collaboration of material scientists, chemists and engineers brought about tailoring of air separation processes to the characteristics of the adsorbent within the constraints imposed by the compression equipment.

Cyclic adsorption processes are described mathematically by a set of coupled non-linear partial differential equations and algebraic equations. Each cycle operates as an unsteady transient, while the overall process must achieve a cyclic steady state to be viable for continuous operation. While many custom developed models have been developed (requiring sophisticated numerical solving routines), the tools have matured to the commercial level with the availability of Aspen Adsorption™ (Aspentech), gPROMS (PSE), ProSim DAC (PROSIM) and COMSOL Multiphysics® (COMSOL) software. The former two offer adsorption templates to facilitate the step-wise building of the governing equations for a given process flowsheet. All have imbedded high level numerical solvers and graphical user interfaces. While these modeling tools greatly facilitate simulation of cyclic adsorption processes, they are dependent upon accurate input data and sub-models for multicomponent isotherms, heats of adsorption, pressure drop and mass and heat transfer coefficients, etc. The simulation of breakthrough experiments can be utilized to extract rate coefficients. Various strategies for modeling cyclic adsorption processes can be found in the literature.

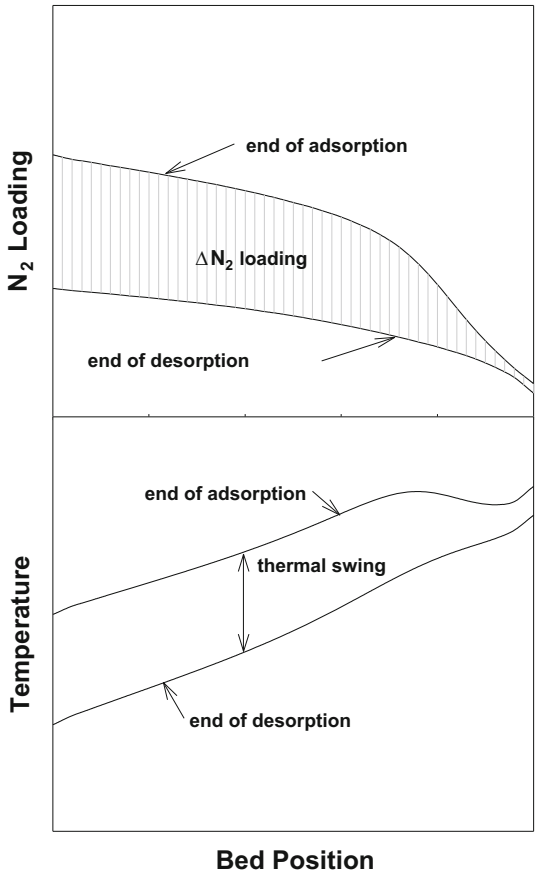

Fig. 8 N_2 loading and thermal gradients in the adsorbent bed

Accurate description of the adsorption thermodynamics is critical to representative modeling of the process. Pure gas isotherms can be measured by several different methods, while obtaining multicomponent (coadsorption) data is more challenging. The loading ratio correlation (LRC) isotherm model developed by Leavitt (Yon and Turnock 1971) for molecular sieve adsorbents utilizes pure gas data to construct a multicomponent isotherm model (including isosteric heats of adsorption) that can be incorporated into the software mentioned above. Sircar (1991) developed a heterogeneous Langmuir model that has recently been applied to N_2 and O_2 adsorption on LiLSX adsorbent (Wu et al. 2014a). Other applicable models can be found in the literature.

Industrial scale adsorbers for air separation behave adiabatically with respect to heat transfer to the environment. Small scale oxygen concentrators are neither adiabatic nor isothermal. In either scale, thermal effects are important and must be included in modeling and

simulation. The bulk separation of air results in a large amount of N_2 adsorbed and the evolution of heat. Desorption of this N_2 (endothermic) during regeneration results in the extraction of heat (refrigeration effect) from the bed and purge gas (Collins 1977). This refrigeration is partially stored in the pre-treatment layer and is returned to cool the feed air as it passes through this layer in the following feed step. The net result is that the pre-treatment layer acts as a thermal regenerator. When combined with the heat released by adsorption of N_2 and O_2 in the main adsorbent layer, these effects result in thermal gradients throughout both the pre-treatment and main adsorbent layers. While the adsorption of H_2O and CO_2 in the pre-treatment layer are also exothermic, their effect upon the thermal gradients is small due to the small amounts adsorbed from air, i.e. relative to the large quantities of N_2 and O_2 adsorbed in the main adsorbent layer. The temperature increases along the main adsorbent layer from feed end to product end and the average temperature of the bed is higher at the end of adsorption than at the end of desorption as illustrated in Fig. 8. This creates a condition known as an "adverse thermal swing" in that the higher temperature during feed reduces the N_2 capacity and the lower temperature during regeneration inhibits N_2 desorption (resulting in a higher (permanent) residual amount of N_2 adsorbed in the bed). An excellent discussion of these effects has been provided by Wilson et al. (2001). These thermal effects, combined with the mass transfer resistance effects and pressure ratio, are the primary determining factors in the N_2 "working capacity" of the adsorbent.

N_2 capacity and N_2/O_2 selectivity have long been measures of adsorbent effectiveness for air separation, e.g. Chao (1989). However, rating an adsorbent's capacity for N_2 at a single adsorption pressure and relying on a definition of selectivity related to distillation theory are totally inadequate for understanding adsorption in a cyclic process. Neither N_2 nor O_2 are completely desorbed in PSA air separation processes, i.e. there remains a substantial residual amount of N_2 and O_2 at the end of the desorption step. The amount of N_2 transacted on and off of the adsorbent bed during each cycle at cyclic steady state is represented by the ΔN_2 loading or N_2 working capacity (Wankat 1986) as illustrated in Fig. 8. The left and right ends of these distributions represent the feed end and product end of the main adsorbent layer. Most of the N_2 working capacity is generated in the equilibrium zone of the bed, while the sharp decline in N_2 loading near the end of the bed occurs in the mass transfer zone (MTZ) where there is a corresponding sharp decline in the N_2 gas concentration. The ΔO_2 working capacity (relatively much smaller than ΔN_2, but still significant) shows less temperature dependence in the equilibrium zone and a much larger concentration dependence in the MTZ (Ackley 2000). The "working selectivity" is related to the separation factor $\Delta N_2/\Delta O_2$. These temperature and loading distributions become evident from detailed modeling and simulation and provide valuable insight to process operation and performance. It is possible to approximate these parameters from the pure gas isotherms and process pressures and temperatures – at least for the contributions in the equilibrium zone. Such approximations are the basis for several different adsorbent screening evaluations, e.g. Maring and Webley 2013; Rege and Yang 2001; Ackley et al. 2003b. These and other techniques have also been used to expose the different thermal characteristics of various N_2-selective zeolites and apply these results to layer different zeolites in the main adsorbent zone according to each material's optimum working capacity and working selectivity (Watson et al. 1996; Notaro et al. 1997; Wilson and Webley 2002; Ackley 2000). The somewhat unique low temperature characteristics of NaX were exploited for improved air separation through externally applied refrigeration (Izumi 1989) and self-refrigeration (Leavitt 1992).

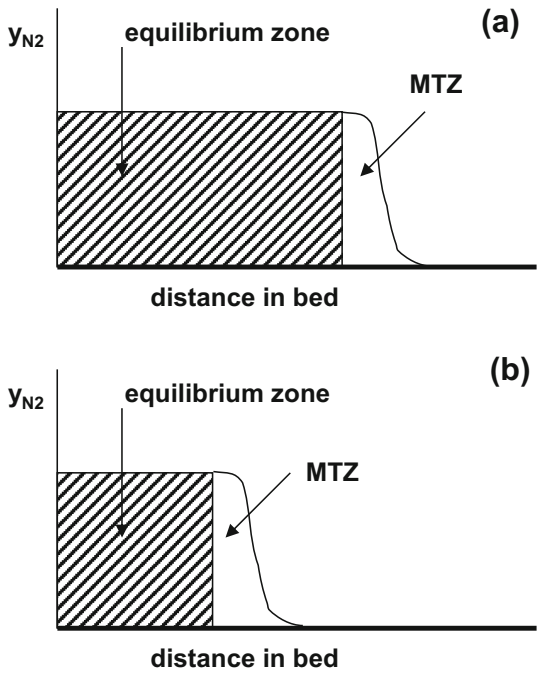

Fig. 9 Equilibrium and mass transfer zones **a** long cycle **b** short cycle

4.2.1 Intensification

While intensification has been an important factor in reducing the size of industrial air separation systems, it is particularly relevant to MOCs and essential to the development of POCs. The concept of the MTZ is inherent in the intensification of adsorption processes. Adsorption of N_2

within the nanoscale cavities or micropores of a zeolite is preceded by diffusion through the macropores of the agglomerated adsorbent particle. This pore diffusion combined with other transport resistances results in a MTZ that travels through the bed leaving behind a zone saturated in the adsorbate (equilibrium zone) as illustrated in Fig. 9a. Adsorption occurs within the MTZ as the concentration of N_2 decreases from that in air to a much lower concentration in the product. The mass transfer front develops rapidly in systems having favorable isotherms (Ruthven 1984), is self-sharpening and reaches a constant pattern that moves through the bed at a constant velocity slower than the gas velocity.

While the constant pattern mass transfer front is an idealized concept, it is very useful in estimating the size of the MTZ and length of unused bed (LUB) for gas adsorption systems (Collins 1967; Lukchis 1973; Wankat 1986). It is apparent from Figs. 8, 9a that the bed utilization increases as the length of the bed (L) increases with respect to the fixed length of the MTZ (L_{MTZ}). Lukchis (1973) suggests that 90% of the maximum equilibrium capacity of the bed is reached when $L/L_{MTZ} \geq 5$. The general concept of reducing adsorbent inventory by decreasing bed length with a corresponding reduction in cycle time (Fig. 9b) is one form of intensifying the system. For a given system, however, this results in a reduction in L/L_{MTZ} and a loss in working capacity and O_2 recovery, i.e. L_{MTZ} remains fixed as the equilibrium zone shrinks. The validity of early studies ignoring mass transfer effects depend upon the condition $L >> L_{MTZ}$. The reduction in cycle time in combination with various intensification strategies described below is largely responsible for the reduction in BSF of commercial industrial air separation systems from $\geq$ 1000 TPDO (Reiss 1994; Kumar 1996) to $\leq$ 400 TPDO (Ackley and Leavitt 2002; Ackley et al. 2003c).

A dimensionless model was formulated for intensification of adsorption processes wherein the intensified process preserves performance in terms of product purity, O_2 recovery and pressure drop while increasing adsorbent productivity (Wankat 1987, 1990; Rota and Wankat 1990). This model requires L_{MTZ} to be reduced in proportion to the reduction in L to maintain the same L/L_{MTZ} ratio, as well as making other changes (e.g. bed area) to maintain the same pressure drop (ΔP) across the bed as in the original system.

In order to fully appreciate the concept of intensification it is instructive to review the relationships for bed pressure drop and mass transfer rate. The Ergun equation (Ergun 1952) provides an accurate convenient representation for bed pressure drop for use in process modeling (Todd and Webley 2005b):

$$\frac{\Delta P}{L} = \frac{150 u_0 \mu}{(\phi_s d_p)} \frac{(1-\varepsilon)^2}{\varepsilon^3} + \frac{1.75 \rho u_0^2}{\phi_s d_p} \frac{(1-\varepsilon)}{\varepsilon^3} \tag{2}$$

ρ is the gas density, g is the gravitational constant, ε is the bed void fraction, d_p is particle diameter, ϕ_s is the sphericity of particles, μ is the gas viscosity and u_0 is the superficial gas velocity. The mass transfer from the fluid stream to the adsorbent particle can be represented by the linear driving force (LDF) model (Glueckauf 1955):

$$\rho_b \frac{\partial \bar{w}_i}{\partial t} = k_i (c_i - \bar{c}_{s_i}) \tag{3}$$

where w_i is the average molar loading of adsorbate i, ρ_b is the adsorbent packing density, k_i is the mass transfer coefficient, c_i and c_{si} are the average molar adsorbate gas phase concentrations in the bulk fluid and inside the particle macropores (in equilibrium with the adsorbate loading), respectively. The term inside the brackets is the "concentration driving force." A corresponding relationship can be written in terms of an adsorbent loading driving force, recognizing that the value of k_i will be different. The lumped parameter k_i can be partitioned into the possible mass transfer resistances of film, micropore diffusion and macropore diffusion as described in Eq. 4 (Ruthven 1987):

$$\frac{1}{kK} = \left(\frac{r_p}{3k_f}\right) + \left(\frac{r_p^2}{15\varepsilon_p D_p}\right) + \left(\frac{r_c^2}{15KD_c}\right) \tag{4}$$

r_p is the adsorbent particle radius, r_c is the zeolite crystal radius, ε_p is the particle void fraction, k_f is the film mass transfer coefficient, K is the Henry Law constant, D_p and D_c are the macropore and micropore diffusivities, respectively. Various formulations of Eqs. 3 and 4 may contain the parameters K, τ (tortuosity) and/or ε depending upon the formulation of diffusivity and the units of measure of the other terms in the equations. For the purpose of modeling and simulation, the lumped mass transfer coefficients k_i are sufficient and can be determined by several different methods, e.g. breakthrough tests. It is beneficial, however, to understand the underlying controlling mechanisms for mass transfer when performing intensification.

The dominant term for air separation using N_2-selective type X zeolites is the macropore diffusion (middle term on the right hand side of Eq. 4). While the film resistance ($r_p/3k_f$) is typically not negligible, it is generally small in comparison to the macropore diffusion. Diffusion in the micropores (last term in Eq. 4) is very fast compared to macropore diffusion in large pore zeolites. While the macropore vs. micropore diffusion control debate occasionally resurfaces, numerous studies using different models and experimental techniques confirm macropore control for permanent gas diffusion into large pore zeolites, e.g. Hu et al. 2014; Kikkinides and Politis 2014b; Todd and

Webley 2005a. The usual test to distinguish between micropore and macropore diffusion in an adsorbent is to perform breakthrough tests with different particle sizes of the adsorbent. The breakthrough curve sharpens with smaller particle diameter for macropore control (k_i increases), while the breakthrough characteristic remains relatively independent of particle size in micropore control. This test has been demonstrated for N_2 adsorption on the small pore natural zeolite clinoptilolite (Ackley et al. 2003b).

The benefit of the above analysis is that the mass transfer rate coefficient can be represented by the middle term in Eq. 4:

$$k_i \cong \frac{15\varepsilon_p D_{p_i}}{r_p^2} \tag{5}$$

This relationship offers several strategies for increasing rate by manipulating the physical characteristics of the adsorbent particle for the purpose of intensifying the process, i.e. k_i is inversely proportional to the square of the particle radius (r_p) such that rate increases (L_{MTZ} decreases) as particle size decreases, while k_i increases with increasing ε_p and D_p. The primary means employed to reduce L_{MTZ} has been to decrease the adsorbent particle size (recognizing the inverse relationship between adsorption rate and the square of the particle diameter (d_p^2)).

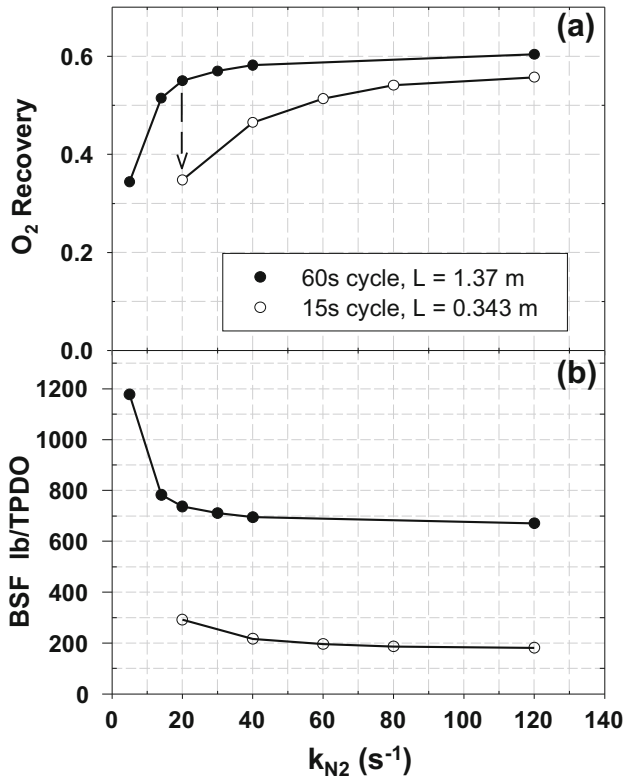

Fig. 10 Effects of rate upon O_2 recovery and BSF

However, smaller particles result in higher bed ΔP. Varying degrees of productivity improvement were accomplished while utilizing different strategies to control bed ΔP (Miller 1990; Hirooka et al. 1992; and Hay et al. 1993).

Equation 5 also suggests that rate can be increased by increasing the particle porosity. This has been suggested in several studies including the combination of large pore adsorbents with intraparticle convection (Lu et al. 1992; Lu and Rodrigues 1993) and increased porosity of 0.38–0.60 in zeolites (Moreau and Barbe 1997). The typical range of particle porosity for commercial clay-bound adsorbents has been 0.30–0.38 (Wankat 1990), and more recently suggested to be 0.35–0.40 (Zheng et al. 2014). The simple reason for the narrower practical ranges is that porosity is inversely proportional to density and density is directly related to particle strength—high density (low porosity) results in lower diffusivity and low density (high porosity) particles have low crush strength. Furthermore, higher porosity/lower density adsorbent requires a larger volume of adsorbent for the same N_2 working capacity per unit mass of adsorbent.

The third option is to enhance the rate by increasing the intrinsic macropore diffusivity (D_p) of the adsorbent (Ackley and Leavitt 2002). Increasing D_p avoids the disadvantages associated with smaller particles and higher porosity. Improving the macropore geometry is a more difficult path and may require a different binder type and/or binder physical properties, as well as modified processing methods. Controlling the macropore geometry throughout the various zeolite manufacturing steps of synthesis, agglomeration, ion exchange and calcination/drying can be challenging. D_p is not a directly measureable parameter but can be calculated from Eq. 5 once k_{N2} is determined. Traditional adsorbents used in air separation were shown to have a narrow range of D_p. Various strategies have been employed to more than double D_{pN2} over that of traditional adsorbents (see discussion above in Sect. 4.1.1), resulting in a corresponding increase in N_2 mass transfer rate k_{N2}. The effects of increasing k_{N2} upon O_2 recovery and BSF while reducing cycle time and bed depth are shown in Fig. 10 (Ackley and Leavitt 2002). Reducing the cycle time and bed depth without increasing rate, i.e. reducing L without reducing L_{MTZ} results in a less than proportionate decrease in BSF. This is illustrated in Fig. 10 for a four-fold reduction in cycle time (at $k_{N2} = 20\ s^{-1}$) producing only about a two-fold reduction in BSF due to the fact that a significant reduction in O_2 recovery occurs. This undesirable effect can be mostly overcome by increasing k_{N2} (reducing L_{MTZ}). There is a diminishing return in performance (at a fixed cycle time) at very high values of k_{N2}, i.e. L/L_{MTZ} approaches a constant value.

An alternate form of intensification is termed RPSA. This method employs very small particles (0.1–0.4 mm) in

a process in which the feed step is far removed from the MTZ concept discussed above, i.e. the mass transfer front travels back and forth in only a small portion of the bed, never reaching a constant pattern and only a small portion of the bed capacity is used (Wankat 1986). The process is characterized by very fast cycles (feed step $\leq$ 2.0 s, depressurization times 5–20 s), high feed velocity, high pressure and high bed pressure drop (8–12 psi/ft). The high pressure drop/short cycle combination is necessary to establish optimum bed permeability and internal purging of the adsorbent which operates to generate product continuously using type 5A zeolite (Earls and Long 1980; Jones et al. 1980). This "original RPSA" cycle described in these early patents is distinct from conventional air separation processes, i.e. primarily in the high ΔP per unit bed length ($\geq$ 8 psig/ft vs. $\leq$ 1.0 psig/ft in conventional cycles), the type of cycle steps and the small size of particles used (typically $\leq$ 0.4 mm). Alpay et al. (1994) studied the effects of axial dispersion by modeling these types of RPSA cycles and found the optimum particle size to be in the range of 0.2–0.4 mm.

4.2.2 Pressure ratio and pressure drop

Pressure ratio (P_H/P_L) is determined from the pressures at the end of the feed step (P_H) and at the end of the desorption step (P_L). These end pressures establish the boundaries for the N_2 and O_2 working capacities. The relative shapes of the N_2 and O_2 isotherms result in a decrease in O_2 recovery (and selectivity) as P_H/P_L decreases (Rege and Yang 1997), i.e. the N_2 loading for LiX (concave isotherm) decreases more over the same pressure change ($P_H \rightarrow P_L$) than the O_2 loading (linear isotherm). Selecting P_H, P_L and P_H/P_L is a compromise between O_2 recovery and energy consumption, all within the constraints of the available compression equipment (Smolarek et al. 2000). Compressors and vacuum pumps are typically available in limited pressure ranges dependent upon the number of stages and frame size. Roots type blowers have been the mainstay for industrial air separation, however, this type of equipment is not applicable to POCs. Most air separation processes today utilize single stage equipment to minimize the cost of power and capital.

For a given air separation system, reduction in pressure ratio requires a reduction in cycle time due to the decrease in O_2 recovery. As a result, advantages in energy consumption and BSF are partially offset. This is similar to what happens when cycle time and bed depth (adsorbent inventory) are decreased at a given pressure ratio. Therefore, the intensification principles described above can be applied in the low pressure ratio scenario to compensate for the loss in O_2 recovery while maintaining O_2 production rate and even decreasing BSF. A high rate LiX adsorbent was utilized in a VPSA air separation process within the range $1.5 \leq P_H/P_L \leq 5.0$ to demonstrate decreased unit process power (as low as 7.5–8.5 kW/TPDO) and BSF ($<$ 500 lb/TPDO) at the expense of O_2 recovery with optimum performance achieved at $P_H/P_L \approx 3.0$ (Ackley et al. 2003c). Overall plant power is typically $\approx$ 10 kW/TPDO. These same strategies apply to POC cycles where battery life (power consumption), BSF (concentrator size and weight) and O_2 recovery are important.

The primary resistance to flow in the system is the pressure drop across the adsorbent bed, although valves and other equipment in the system also contribute to pressure loss. Bed ΔP is to be minimized primarily for the following two reasons: (1) larger bed ΔP requires a higher feed pressure and larger compressor for a given desired O_2 product pressure resulting in greater power consumption and increased capital; and (2) a larger pressure gradient in the bed results in a decreasing local pressure ratio along the bed and a corresponding decrease in the local O_2 recovery from inlet to outlet of the bed.

It is evident from Eq. 2 above that higher superficial gas velocity, smaller particle diameter and lower bed void fraction all contribute to increased bed pressure drop per unit bed length. Bed ΔP can be managed within limits by increasing the flow area (decreasing the gas velocity) and decreasing the bed depth. The manufacturing and shipping limits of large diameter cylindrical beds can be extended by the use of radial flow adsorbers. Fluidization limits must be observed in industrial scale air separation, while the small adsorbers used in MOCs can be easily prevented using bed constraint.

4.2.3 Bed packing

Packing the adsorbent in the bed is often given little attention, particularly in small scale laboratory studies. A densely packed bed minimizes adsorbent settling and wall channeling, localized fluidization and attrition. Bed porosity also increases near the wall and can impact the average porosity (and packing density) for bed diameter (D) to particle diameter (d) ratio $<$ 10 (de Klerk 2003). While it might seem tempting to increase ε to reduce bed ΔP, uniformity of flow and long term stability favor a packed bed with maximum fractional density $(1 - \varepsilon)$. "Maximum fractional density" here refers to a bed of randomly packed spheres of uniform diameter wherein the minimum porosity $\varepsilon \approx 0.37$. The fractional density is the ratio of particle volume to bed volume as shown in Eq. 6:

$$(1 - \varepsilon) = \frac{\rho_b}{\rho_p} \tag{6}$$

where ρ_p is the particle density. While synthetic zeolite adsorbents were first produced as extrudates, the preferred form is now spherical beads.

A common misperception is that smaller particles pack more densely than larger particles. Randomly packed monodisperse spheres pack to the same limits stated above independent of diameter. Packing density increases as the particle size distribution becomes more polydisperse – allowing smaller particles to fill the voids between the larger particles. The ratio of the diameters of the largest (d_m) to smallest (d_s) particles within the majority of the distribution, e.g. 95% of the particles between the specified mesh sizes, reflects the degree of polydispersity of the distribution. Most commercial zeolite adsorbents are supplied with the majority of the beads falling within a mesh size range such that $d_m/d_s \leq 2$. It has been shown that for particle size ratios ≤ 3 there is minimal increase in packing fraction over that for randomly dense packed spheres of uniform diameter (German 1999). Thus, a randomly dense packed bed of adsorbent beads with $0.34 \leq \varepsilon \leq 0.37$ is ideal and results in reasonable bed ΔP.

The challenges of dense packing industrial scale adsorbers have been met by various methods, e.g. Nowobilski and Schneider 1994. Such methods are an extension of an early "gravity filling" technique designed for small diameter adsorbent beds (Goshorn and Gross 1943; Gross 1949). These original methods can be easily adapted for filling concentrator beds. Dense packing coupled with bed constraint (Pritchard and Simpson 1986) is particularly important for POC beds that are characterized by a high ratio of wall area to adsorbent volume, are in constant motion with the user and may undergo various orientations during transport.

4.2.4 Endspace void volume

Void space between the control valves and the ends of the adsorbent bed decrease the efficiency of the process, e.g. feed endspace voids result in gas being compressed but not processed through the bed, thereby decreasing O_2 recovery and increasing power consumption (Celik et al. 2012). This problem is particularly restrictive to intensification of industrial scale air separation due to the large volumetric air flows and the correspondingly large pipe diameters (Ackley and Leavitt 2002). It is recommended to maintain endspace to bed volume ratio $\leq 30\%$ to minimize these effects – particularly important on the feed side of the bed. This condition should be easier to control in the small scale of POCs where volumetric flows are quite small. Many of the POC patents (discussed below) describe molded bases and endcaps that include well-designed flow channels connecting beds and valves.

4.2.5 Heat transfer

Heat transfer affects the local thermal conditions within an adsorbent bed. These effects can be particularly significant in bulk separation, fast cycle and thermal swing adsorption processes. Process modelling and simulation require determination of heat transfer coefficients. Tsotsas and Schlundler (1990) address the complex heat transfer mechanisms within a packed bed. The selection of an appropriate model is critical in that different correlations can result in heat transfer coefficients that differ by one or more orders of magnitude. A full discussion of this subject is beyond the scope of this review. As a result, only a few practical guidelines are offered here as it relates to air separation.

For modeling of air separation processes, the wall heat transfer coefficient (H_w) and the particle to fluid heat transfer coefficient (H_{pf}) are generally adequate. Industrial scale adsorbers operate adiabatically such that $H_w \approx 0$. Small scale adsorbers such as used in laboratory and pilot testing and in concentrators are neither adiabatic nor isothermal. These "non-isothermal" adsorbers exchange heat with the environment. Despite attempts to control such processes in an isothermal mode, the time scale for heat transfer is much slower than that for mass transfer, resulting in thermal gradients and waves within the bed even when small diameter beds are immersed in a thermal bath. H_w is essentially a lumped parameter representing several mechanisms within the bed and care must be exercised in selecting a useful correlation (Tsotsas and Schlundler 1990). Various correlations can be applied for estimating H_{pf}, e.g. Martin 1978; Bird et al. 1960.

For the case of POCs, a cooling fan is usually recommended due to the heat generated by the compressor and/or vacuum pump. This heat and the heat of compression may further impact the thermal conditions inside the concentrator beds.

5 Progress in air separation technology: medical O_2 concentrators

Important fundamental concepts fueling the advances in air separation technology (adsorbents and process development) have been driven by industrial air separation (as summarized above in Sect. 4). Most, if not all, of these concepts are not only applicable but also critical to achieving optimum performance in MOCs. Attention is now focused upon adsorbents and specific process studies directed to the improvement of MOCs.

Table 6 Oxygen concentrator NaX adsorbents

Manufacturer	Product	Zeolite	Particle size	Bulk density (kg/m^3)	N_2 Capacity[a] (ml/g)	H_2O content wt %
Arkema (Ceca)	NITROXY® 5	NaX	≈ 0.60 mm	580–640	8.0	1.0
Honeywell (UOP)	OXYSIV™ 5XP	NaX	0.55 mm	700		0.5
Jalon[b]	JALOX- 501	NaX	20 × 50	≥ 620	≥ 8.0	
Zeochem®	ZEOX® O_{II}	NaX	0.4–0.8 mm	660	8.7	

[a]Determined at 1atm and 25 °C

[b]Also known as Luoyang Jianlong Micro-nano New materials Co., Ltd

Table 7 Oxygen concentrator LiX adsorbents

Manufacturer	Product	Zeolite	Particle size	Bulk density (kg/m^3)	N_2 Capacity[a] (ml/g)	H_2O content (wt%)
Arkema (Ceca)	NITROXY® Revolution	LiX	≈ 0.40 mm	580–640	18.5	1.0
	NITROXY® SXSDM	LiX	≈ 0.60 mm	580–640	20.0	1.0
Honeywell (UOP)	OXYSIV™ MDX	LiX	0.4 mm	610		0.5
			0.6 mm	620		0.5
Jalon	JALOX-101	LiX	20 × 50	630 ± 30	≥ 22.0	≤ 0.5
Zeochem®	ZEOX® Z12-07	LiLSX	0.4–0.8 mm	630	23	
	ZEOX® Z12-49	LiLSX	0.4–0.8 mm	600	25	
	ZEOX® OP-32	LiLSX	0.4–0.8 mm	670	26.5	
	ZEOX® OP-92	LiLSX	0.4–0.8 mm	600	26.5	

[a]Determined at 1 atm and 25 °C

5.1 Adsorbents

Both NaX and LiX type adsorbents are currently manufactured for concentrator applications. Typical specifications for commercially available NaX and LiX adsorbents have been compiled in Tables 6 and 7, respectively.[4] The "zeolite" designation given in the tables is that used by the manufacturer and is repeated here to define the class of material only. Specific zeolite composition in terms of Si/Al, degree of ion exchange, type and % binder, etc. is not disclosed by any of the manufacturers. N_2 capacity is represented as a single point on the N_2 isotherm. The N_2 capacity of the Zeochem® adsorbents is greater than adsorbents of the other manufacturers. While the particle diameter range spans 0.3–0.8 mm for all materials, it appears that the average particle size is in the narrower range of 0.4–0.6 mm. The manufacturers did not indicate which method or temperature was used to determine H_2O content, but the Karl Fischer titration method (KF H_2O) is preferred.

Although it is difficult to rate these materials based upon the information provided, it is a safe assumption that many reflect some degree of one or more of the improvements cited in Sect. 4.1.1 above, i.e. reduced Si/Al, high Li exchange, improved binder, higher N_2 capacity, higher N_2/O_2 selectivity and/or higher intrinsic rate.

The NaX adsorbents listed in Table 6 are advertised for O_2 production, although these adsorbents are also applicable for pretreatment to remove H_2O and CO_2. NaX is generally an inferior adsorbent for O_2 production, but may satisfy the need for simpler cycles and/or for older concentrators still in service. The LiX materials listed in Table 7 clearly differ in bulk density and N_2 capacity, likely to be reflected in a difference in the characteristics of the N_2 and O_2 isotherms. Thus, the optimum concentrator cycle may vary for the different LiX adsorbents, e.g. depending also in part on the selection of P_H, P_L and the type of compressor and/or vacuum pump as discussed in Sect. 4 above. Nevertheless, it appears that concentrator manufacturers have a variety of good adsorbent choices.

The price of the adsorbents depends upon quantities ordered and the degree of performance desired. It is expected that a significant premium in price applies to these adsorbents compared to similar larger diameter materials used in industrial air separation. This is largely the result of smaller production batches, lower yield and throughput of smaller particles and the tighter quality

[4] Information in Tables 6 and 7 was extracted from material specification sheets provided by each manufacturer.

control and additional processing steps that may be required for advanced adsorbents for concentrators.

Equilibrium isotherms (pure N_2 and O_2 and their binary mixtures) have been measured for a commercial LiLSX adsorbent (Wu et al. 2014b). The adsorbent was not identified with respect to those materials included in Table 7. Isosteric heat of adsorption was determined as a function of loading, and N_2/O_2 selectivity was computed at various temperatures and pressures. Overall mass transfer coefficients for N_2 and O_2 were determined for the same adsorbent using a dynamic column method (Wu et al. 2014c). Various contributing mass transfer resistances were broken out using literature correlations. It was inferred that more than 60% of the resistance was due to a skin resistance. However, this conclusion is highly unlikely (Moran et al. 2018a) and is probably the result of errors in estimating the other resistance contributors (Rama Rao and Sircar 2017). While isotherms and rates for various sources of LiX may be found throughout the literature, it is recommended that such characteristics should be measured for the specific adsorbent utilized in air separation investigations.

5.1.1 Adsorbent contamination

N_2-selective adsorbents used in fast cycle processes such as POCs are more prone to contamination from moisture due to low BSF, intermittent use, shut down and start up, and ingress from ambient and/or internal diffusion during idle or parked conditions compared to conventional processes (Babicki et al. 2006). Such conditions are exacerbated by the use of structured adsorbents and/or rotary valves – the latter introducing additional sealing issues.

H_2O and CO_2 contamination of adsorbents used in air separation were also studied by Santos et al. (2008). Isotherms for N_2, O_2 and Ar were measured for seven different adsorbents, including Oxysiv^{TM} 5, Oxysiv^{TM} 7 and Oxysiv^{TM} MDX (Honeywell UOP) for use in MOCs. These adsorbents were exposed to H_2O and CO_2 at concentrations typical for air at 5 bar. Regeneration was performed at two temperatures (70 °C and 375 °C) in different environments (dry He, flowing air, evacuation). The level of deactivation was determined by comparing N_2 adsorption capacity before and after exposure to the contaminants. Evacuation at 70 °C followed by pressurization with He appears to be somewhat arbitrary and not representative of typical PSA operating conditions. Some adsorbents were reported to be irreversibly damaged when exposed to non-flowing air at 375 °C in a muffle furnace. Breck (1974) indicates that hydrothermal damage can occur in NaX at temperatures starting at 350 °C. Zeolites with adsorbed H_2O must be calcined and/or dried carefully to remove moisture slowly during thermal processing as demonstrated for various exchanged type X adsorbents (Coe and Kuznicki 1984; Ackley and Barrett 2008). While the high temperatures typical for regenerating zeolites are not representative of those present in air separation, such conditions are often employed to prepare adsorbents for laboratory air separation experiments. Such drying must be performed carefully to insure against damage, as well as to achieve moisture levels $\approx$ 0.5wt%.

5.2 Processes

During the early years of MOC development (from about 1975 to 2000) there were multiple process options available for generating oxygen, i.e. industrial air separation, RPSA processes and other processes customized for MOCs. Many of the early patents were concerned with defining and configuring a much smaller scale system built around the air separation process to deliver O_2 to a patient in their home. Such stationary concepts required the integration of valves, compressors (and/or vacuum pumps), adsorbent enclosures (beds), product tanks, control systems and electronics all packaged appropriately for home use. These components were substantially smaller and different from those used in industrial air separation systems. Examples of patented MOC systems include those for apparatus/enclosure (McCombs and Schlaechter 1981, 1982; McCombs 1983a), controls (Rowland 1985) and various bed configurations (McCombs 1983b, 1989).

VPSA single bed processes utilizing one compressor to provide both pressurization and evacuation have been patented. Kratz and Sircar (1984) utilized a synthetic Na-mordenite in a 90 s 5-step cycle to produce 90% O_2 at a recovery of 55–60%. The process included a pretreatment layer and operated with a high pressure ratio ($P_H/P_L \geq 8.6$). A simple 2-step cycle utilizing 10 lb 13X adsorbent with O_2 production of 4–5 lpm and operating between $P_H = 2.8$ psig and $P_L = -2.4$ psig was claimed by Schlaechter (1985).

Shin et al. (2000) was motivated to study "incomplete equalization" as practiced in a commercial stationary concentrator. Both experiments and modeling were performed assuming isothermal conditions with negligible pressure drop. A two-bed, six-step cycle of 160 s with 13X adsorbent (0.4 mm–1.0 mm) was investigated at a pressure ratio of about 3.0 using various extents of equalization. While maximum recovery was observed at complete equalization, productivity increased with incomplete equalization. The number of spatial points were selected in the model to reconcile the model and experiment results – necessary to compensate for the absence of kinetic effects in the model. While this strategy is not recommended, it does draw attention to the fact that numerical dispersion can masquerade as real dispersion in the process and it is

important in modeling to choose small enough spatial step sizes to avoid this condition.

Jee et al. (2001) investigated a two-bed, six-step cycle using 13X (20 × 32 mesh) for $3.0 < P_H/P_L < 6.0$. Cycle times of 26 s and 36 s were performed by varying the length of the adsorption and purge steps. Top-to-top equalization was included. The O_2 concentration profiles in the bed suggest that the MTZ occupies 40–50% of the bed length, which would be consistent with a slow adsorption rate resulting from the very low particle porosity reported ($\varepsilon_p = 0.21$).

5.2.1 Original "RPSA" processes

According to Cassidy and Holmes (1984), the original class of RPSA systems (characterized by high bed ΔP per unit bed length as described in Sect. 4.2.1 above) were applied in MOCs in 1979. These systems for MOCs were derived from concepts described in patents (Earls and Long 1980; Jones et al. 1980) and represented short cycles (< 3 s) and small diameter particles. A three-bed system improvement included a discontinuous feed and lengthened re-pressurization step to increase the feed pressure using 40 × 80 mesh 13X adsorbent (Dangieri and Cassidy 1983). Kaplan et al. (1989) presented a three-bed RPSA process (2.4 s cycle time) aimed at stationary concentrators with a substantial reduction in BSF compared to commercial concentrators and industrial air separation plants at that time, i.e. 200 TPDO compared to 970 TPDO and 2900 TPDO, respectively. O_2 recovery varied from about 25% to 30% at 90% O_2 depending upon the feed pressure (pressure ratio). The smallest BSF (≈125 lb/TPDO) for this class of RPSA systems utilized a complex arrangement of six beds coupled to a rotary valve (Kulish and Swank 1998). The adsorption step (1–2 s) and desorption step (5–10 s) comprised a cycle with $P_H/P_L = 3.0$ to produce 5 lpm O_2 with only about 1.3–1.4 lb adsorbent. Pritchard and Simpson (1986) designed and built a single bed prototype using 60 × 80 mesh 5A zeolite and a 5.7 s RPSA cycle to produce > 85% O_2 in a conventional concentrator, or alternatively to produce 0–2 lpm of 30% O_2 for an incubator in neonatal applications. All of these systems were aimed at reducing the size of MOCs, particularly for stationary concentrator applications. It is unclear how widely such RPSA cycles were commercialized, but none of these cycles appear to be used in the current equipment in Sect. 3 above.

A high frequency pulsed PSA (PPSA) was investigated for application in POCs (Rama Rao et al. 2010). A single bed, two-step process was simulated using an isothermal model with varying particle size (0.01–0.4 mm), bed length (0.4–600 cm) and feed pressure (1.5–10.5 atm). The maximum O_2 recovery determined for 5A and AgLiX adsorbents was ≤ 25% and ≤ 50%, respectively, at a particle diameter to bed length ratio (d_p/L) of about 1×10^{-4}. A matrix of conditions for $d_p = 0.02$ mm, $P_H/P_L = 3.5$ atm and varying cycling frequencies (0.04 – 7.5 Hz) was generated to satisfy the POC operating conditions of 5lpm and 90% O_2 product purity. In a follow-up experimental study of this process using small diameter 5A particles (63–75 μm), the maximum O_2 product purity that could be achieved was limited to < 40% (Rama Rao and Farooq 2014a). The authors attributed this result to very high pressure drop from clustering of particles and the effects of axial dispersion.

"RPSA" has recently been applied to describe fast cycle conventional air separation processes—intensified fast cycle processes that have largely been developed for application to POCs as discussed in Sect. 5.2.3 below. However, this duality in process terminology makes the use of the term "RPSA" less meaningful without a more specific definition of the process conditions.

5.2.2 Intensification

The Wankat (1987) intensification methodology utilizes scaling rules to shrink an optimum performing adsorption process without diminishing its performance. BSF is reduced by cycling faster while O_2 purity, pressure drop, power consumption and O_2 production capacity remain unaffected. However, large industrial scale air separation processes reach a practical intensification limit due to the increase in the inlet void volume to bed volume ratio and switching times of large size valves. The piping and valve sizes cannot be proportionately decreased with the bed size because of the large volumetric flow rates characteristic in the industrial scale processes. MOCs and POCs operating at much lower O_2 production capacity and volumetric air flow rates are not similarly limited. As a result, it is possible to intensify the concentrator air separation process to much lower cycle times.

The strategy to combine small particles with higher intrinsic macropore diffusivity to intensify industrial air separation (Ackley and Leavitt 2002) was extended to POCs with very fast cycles (Ackley and Zhong 2003d). A BSF of 50 lb/TPDO was demonstrated for a 5.0lpm O_2 production rate and 0.5 lb adsorbent through both modeling and experiment using a high rate LiLSX adsorbent (X-2) in a VPSA cycle with $P_H/P_L = 3.0$. An O_2 recovery of 60% (similar to that in industrial scale processes with BSF = 350 lb/TPDO) was achieved with a six-step cycle, L = 4.0 in and a total cycle time of 4.0 s. Reductions in BSF were also demonstrated for a PSA cycle (X-2 adsorbent) and for PSA and VPSA cycles using commercial adsorbent Oxysiv™ 7 (Honeywell UOP). The average particle diameter of both adsorbents was ≈ 0.55 mm.

These results were compared with those from other studies previously discussed and with commercial stationary concentrator technology (typical in 2001) in Fig. 11 (Ackley 2003a, d).

Zhong et al. (2010) considered the simultaneous effects of axial dispersion and macropore diffusion at various interstitial velocities and particle diameters for LiLSX. Using a simplified isothermal process model, it was shown that pore diffusion dominates for $d_p \geq 1.0$ mm, while axial dispersion becomes increasingly important at smaller particle sizes until it begins to dominate for $d_p < 0.1$–0.3 mm. The parameter $k_{N2}/\Delta P/L$ is maximized (mass transfer resistance and pressure drop per unit bed length are minimized) in the particle diameter range of 0.3–4 mm, depending upon the flow velocity. Detailed non-isothermal and pore diffusion models were then applied to determine the impact upon air separation performance (BSF, O_2 recovery and power consumption) as a function of particle diameter (including the simultaneous influences of axial dispersion, pore diffusion and $\Delta P/L$). It was shown that it is possible to intensify the process to achieve BSF < 50 lb/TPDO, cycle times < 4.0 s (> 0.25 Hz) and L < 100 mm for $0.10 < d_p \leq 0.50$ mm while maintaining O_2 recovery ≥ 50%.

The importance of axial dispersion has been further supported by the modeling and breakthrough studies of Moran et al. (2018a). Axial dispersion must be estimated from correlations that predict the value of the dispersion coefficient (D_L). A rigorous analysis demonstrated the importance of choosing the correct correlation. It was also shown that the effects of axial dispersion and macropore diffusion for LiLSX particles ($d_p = 0.5$ mm) were approximately equal, while macropore diffusion was the dominate resistance for 2.0 mm particles. Film resistance was estimated to be contribute about 10% to the overall mass transfer coefficient.

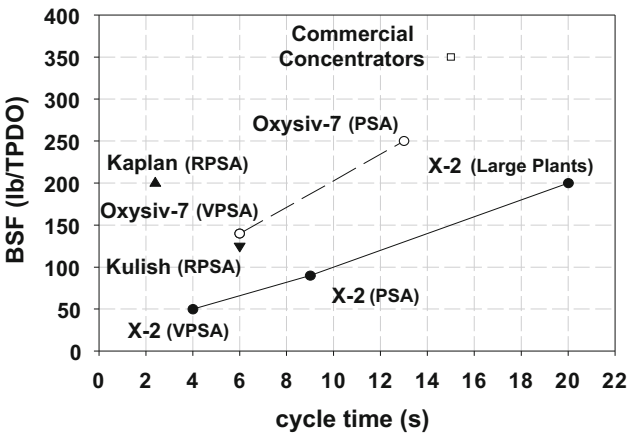

Fig. 11 BSF for RPSA, PSA, VPSA cycles

Moran and Talu (2018b) also studied a two-bed, 4-step rapid VPSA (RVPSA) Skarstrom cycle (no equalization) using a commercial LiLSX adsorbent (0.5 mm particle). Both short (1.09 cm) and long (10.2 cm) beds containing 5.3 g and 5.7 g adsorbent, respectively, were tested for $2.5 \leq P_H/P_L \leq 3.5$ (P_H = 200 kPa). Maximum O_2 recovery was < 20%. BSF was found to decrease with decreasing cycle time to some optimum time upon which BSF then increased at shorter cycle times. BSF minimums ($100 \leq BSF_{min} \leq 250$ lb/TPDO) were observed at cycle times in the range of 3–5 s. These parameters were determined at various superficial velocities, i.e. velocity was increased as cycle time decreased in order to maintain 96% O_2 product purity (argon-free air feed). It was reasoned that macropore diffusion was the primary resistance responsible for the minimum in BSF, although there was a non-negligible contribution from axial dispersion at this particle size. It was further shown that the L_{MTZ} could be approximated as a linear function of the gas velocity. At first this appears to be in conflict with the formulation of the overall mass transfer coefficient where the axial dispersion contribution is directly proportional to the square of the interstitial velocity (Moran et al.2018a; Zhong et al. 2010). These different analyses and the impact upon the MTZ depend upon the level of axial dispersion present at the operating conditions of the device – most importantly the particle size and velocity. Cycle time and adsorbent particle size may vary considerably amongst commercial POCs. Thus, caution must be exercised when selecting representative rate models in process simulation.

5.2.3 RPSA and RVPSA for POCs

The popularity and success of POCs motivated numerous academic studies over the last decade with a variety of objectives aimed at defining processes and conditions for reduced size, weight (adsorbent inventory) and cycle time. By definition, the RPSA investigations below are all concerned with fast cycles and also consider the effects of small particle diameter. However, none of these studies followed the intensification strategy of Wankat (1987). It is emphasized again that these more recent RPSA processes differ from the "original RPSA" processes described in Sect. 5.2.1.

Chai et al. (2011) performed experiments using a PSA Skarstrom-type cycle and a single bed containing 1.0 g Oxysiv™ MDX adsorbent (average particle sizes of 0.35 mm and 0.45 mm). Feed pressures of 2–4 atm (P_L = 1 atm) and cycle times varying from 2 to 10 s were employed to demonstrate BSF minimums occurred in the range of 2–4 s. The BSF_{min} varied with different P_H/P_L and average particle size, but in all cases $BSF_{min} < 70$ lb/TPDO. However, maximum O_2 recovery was limited to ≈

35%. O_2 recovery decreased steeply for cycle times < 5.0 s. Simplifying conditions applied in these experiments included the use of dry, CO_2-free feed air, an independent source of synthetic purge gas (90% O_2), large voids at the inlet and exit of the bed and the absence of any equalization steps.

The role of pressure drop on O_2 recovery and BSF on a two-bed system using LiLSX (0.5 mm) in a six-step VPSA cycle was studied by Moran and Talu (2017). Both short (9.8 cm) and long (19.6 mm) columns each containing 5.7 g adsorbent were tested. The results showed minimal effect of ΔP upon "performance" as cycle frequency increased. The experimental results were supplemented with modeling to show minimal impact of ΔP upon the N_2 concentration fronts and loading distributions. The absence of a pretreatment layer could result in thermal gradients significantly different than in an actual concentrator bed—potentially impacting process performance (Watson, et al. 1996; Ackley 2000). Observed "performance" was limited to BSF (50 to ≈ 160 lb/TPDO) and O_2 recovery (25–50%) for these VPSA cycles. The non-negligible effect of ΔP upon energy consumption was not determined.

The difference in process performance (BSF and O_2 recovery) was measured for two commercial LiLSX adsorbents exhibiting significantly different N_2/O_2 selectivity (Wu et al. 2016). A Skarstrom-type PSA four-step cycle (using pressurization with product O_2 instead of feed air) with $P_H/P_L = 3.2$ was studied for total cycle times varying from 3 to 9 s. The adsorbent with the higher N_2/O_2 selectivity exhibited the highest O_2 recovery (≈32%) and lowest BSF (≈140 lb/TPDO) at the optimum cycle time of about 6 s.

The N_2 desorption efficiency in the back-purge step was evaluated to determine the sensitivity to mass transfer, axial dispersion, pressure drop, non-isothermal and heat transfer effects (Chai et al. 2012). A single purge step (0–2.0 s step time) was modeled by progressively adding the non-ideal factors. The fractional purge required was compared with that determined in an idealized purge step (using 100% O_2 purity for purge) at the same fractional N_2 desorption. The starting condition for purge was a column containing LiX (particle sizes of 0.2 mm, 0.4 mm or 1.5 mm) equilibrated at 298 K, 1 atm with 79% N_2 and 21% O_2. Desorption efficiency was most affected by step time, mass transfer rate, pressure drop, non-isothermal conditions and axial dispersion. Various column length to diameter ratios (L/D) and additional particle sizes (0.10 mm, 0.3 mm diameter) were examined in a follow-up study using the same modeling strategy (Chai et al. 2013). Emphasis was upon fractional N_2 desorption ≥ 80% resulting in gas phase N_2 concentrations in the bed ≤ 0.30 – conditions that suggest significant over-purging of the bed and high O_2 waste. These results were not associated with overall PSA performance.

The effects of various transport resistances upon pressurization and depressurization times were investigated using a single bed of LiX (170 g) (Rama Rao et al. 2014b). The study was carried out similar to the one above by Chai et al. (2012) for the back purge step (Rama Rao et al. 2014c). It was observed that mass transfer resistance and pressure drop were the dominant effects in achieving step times ≤ 1.0 s. While smaller particles increase mass transfer rate (allowing for shorter step times), bed ΔP increases (requiring longer step times to reach the same peak pressure). These competing effects result in a range of minimum step times ≤ 1.0 s observed at $0.2 \leq d_p \leq 0.35$ mm. The effects of L/D upon pressurization/depressurization step times were minimal for L/D ≤ 2.5.

A single bed enclosed within a product collection tank (1.54 l) was suggested for POC applications (Rama Rao et al. 2014d). The adsorbent bed (d_{bed} = 50 mm, L = 127 mm) contained 148 g LiX (Oxysiv™ MDX, Honeywell UOP) with $0.2 \leq d_p \leq 0.6$ mm. Dry, CO_2-free air from a compressed gas cylinder provided the feed to a 4-step PSA Skarstrom-type cycle (P_H = 4 atm, P_L = 1 atm). The effects of co-current feed and countercurrent product pressurization were compared, with the latter providing the better performance. Cyclic steady state was taken at 50 cycles with a maximum temperature variation observed at the bed midpoint of 7 °C—reflecting the lack of the regenerative effect of the pretreatment layer which would have resulted in a much larger ΔT. An O_2 product (90% purity) flow rate of 1.6 lpm was achieved for BSF = 100 lb/TPDO and O_2 recovery = 27% at a cycle time of 5.5 s. The absence of a compressor was evident in the nearly three-fold decrease in the feed air flow rate during the adsorption step, i.e. in contrast to the flow/pressure characteristic of a typical compressor as shown in Fig. 2.

Rama Rao et al. (2015) extended the above study to include LiLSX Zeox® Z12-07 (Zeochem®) ($0.4 \leq d_p \leq 0.8$ mm). An O_2 product (89.3% purity) flow rate of 2.2 lpm was achieved for BSF = 70 lb/TPDO and O_2 recovery ≈ 30% at a cycle time ≈ 5.5 s. After evaluating the isotherms and rate characteristics of both the Oxysiv™ MDX and Z12-07 adsorbents, it was concluded that the adsorbents were comparable despite the differences in average particle size. The BSF and O_2 recovery results, however, are not self-consistent, i.e. a difference in BSF (100 vs 70 lb/TPDO) should have resulted in a similar difference in O_2 recovery because the differences in feed air flow and product purity were relatively small. Furthermore the measured N_2 adsorption loading for Z12-07 at 30 °C and 1 atm (≈ 16.8 ml/g) is significantly lower than the Zeochem® stated N_2 capacity (23 ml/g at 1 atm, 25 °C). Rate

characteristics were determined for a set of conditions quite different than those used in the PSA tests. Thus, the conclusion that the bed ΔP was responsible for the difference in PSA performance is not convincing.

The effects of feed air pressure were examined in the same single bed (enclosed in product tank) and PSA cycle (nominal cycle time of 6 s) described in the studies cited above (Rama Rao et al. 2016). The bed contained 150 g LiLSX (Zeochem®). BSFs (194, 153, 96.7 lb/TPDO), O_2 recoveries (20.3, 21.6, 23.6%) and purge to feed ratio (0.212, 0.183, 0.117) were determined for P_H = 2.7, 3.2 and 4.0 atm, respectively, and 90% O_2 purity.

A rapid VPSA five-step cycle with "intermediate pressurization" (equalization) was investigated using a single bed containing Al_2O_3 (0.02 kg) in a pretreatment layer and LiLSX (0.5 mm) adsorbent (Jalon) in the main N_2-adsorbing layer (Zhu et al. 2017). An auxiliary tank was used to collect product gas following the adsorption step, and subsequently used to partially pressurize the bed prior to feed air pressurization. Additional characteristics included the following: L = 0.28 m, d_{bed} = 30 mm, 0.1 kg LiLSX, P_H/P_L = 3 or 4, P_H = 240 kPa, and cycle times from 5 to 9 s. Experimental results were compared to those from a detailed model with complete energy, momentum and material balances. Correlations were used to estimate the mass and heat transfer and axial dispersion coefficients.[5] The thermal regenerative effects of the pretreatment layer are reflected in the results as they should be. The benefits of the intermediate pressurization are presented in terms of O_2 product purity. Maximum O_2 recovery (30%) and minimum BSF (183 lb/TPDO) were attained for 7 s cycle time, P_H/P_L = 4 and 0.75 lpm O_2 product flow.

The collection of RPSA works in this section support fast cycles ($\leq$ 10 s) and small diameter particles of LiX or LiLSX (0.2 mm $\leq d_p \leq$ 0.8 mm) to achieve BSF $\leq$ 200 lb/TPDO for application in POCs. In view of the well-established performance of industrial PSA and VPSA air separation processes with O_2 recoveries of 30 to 50% and 40 to 60%, respectively, it is disconcerting that most of these studies show low O_2 recoveries $\leq$ 30–35%. This is also surprising in view of the fact that it has been demonstrated that the higher O_2 recoveries can be preserved in POCs through intensification. Furthermore, all of these RPSA investigations incorporate one or more of the following simplifying factors: isothermal, isobaric, no pretreatment layer, use of compressed air rather than actual compressor or vacuum pump – all of which would tend to overstate O_2 recovery. Plausible reasons for such low recovery are the use of PSA cycles instead of the higher performing VPSA processes, the absence of equalization (Skarstrom cycle) and/or product pressurization, over/under purging with O_2 product, excessive endspace void volumes and low N_2 working capacity and N_2/O_2 working selectivity of the particular adsorbent and/or to water contamination. The use of adsorbents with inferior thermodynamic and kinetic properties, as well as experiments conducted at higher O_2 product purity, will also contribute to lower O_2 recovery. None of these published studies determine unit power (W/lpm), which is directly proportional to O_2 recovery and one of the most critical performance variables for POCs.

[5] The correlation for the Peclet No. (Pe_{∞}) is incorrect and should be taken from the original source (Langer et al. 1978).

5.2.4 Process optimization

Optimization of cyclic adsorption processes is quite challenging but offers the opportunity to identify critical parameters required to achieve a desired performance, as well as to reduce the number of process modeling and/or laboratory experiments. This topic was not included in Sect. 4 as its consideration with respect to the breadth of adsorption is beyond the scope of this review. Nevertheless, several studies that have been conducted with the objective to optimize MOCs are briefly discussed here.

An analysis strategy and optimization procedure were developed for VPSA and PSA air separation processes (Cruz et al. 2003). These methods were extended to compare "valveless operation" typical in concentrators, i.e. flows between beds and between product tank and beds determined by the ΔP across orifices with orifice coefficient (C_v) (Santos et al. 2004). A simple four-step cycle (pressurization, O_2 production, depressurization and purge) was studied for three different adsorbents, including Oxysiv™ 5 (NaX) and Oxysiv™ 7 (LiX) available at that time. Optimization variables included dimensionless ratio of pressurization to production step times, ratio of column length to product tank length (volume ratio), and the orifice C_vs for feed, product tank, vent and purge. A pressure ratio P_H/P_L = 3.0 was used for both the PSA and VPSA cases. Model simplifications included ignoring bed pressure drop and assuming isothermal operation. The objective function for operation was constructed around investment cost, operating cost and product value. However, this was reduced to maximizing O_2 recovery after reasoning that the operating costs were negligible in comparison to the investment cost. A somewhat different logic may be required for optimization of POCs. It was concluded that the lowest power and highest O_2 recovery is achieved using VPSA with LiX adsorbent, although a smaller product tank is possible using PSA. Maximum O_2 recovery determined from the modeling was $\sim$ 30% using Oxysiv™ 5 for both PSA and VPSA cycles, while the results for Oxysiv™ 7 were $\sim$ 45% (PSA) and $\sim$ 55% (VPSA). A commercial concentrator (containing Oxysiv™ 5) with similar

characteristics to those in the model and with P_H = 0.3 MPa and P_L = 0.1 MPa was evaluated at different flow rates and found to have an optimum O_2 recovery of ~ 22% at an O_2 product flow rate ~ 4.0 lpm.

A follow-up to the above study was expanded to include a six-step PSA cycle (two-bed) for the purpose of evaluating various equalization schemes, e.g. top–top, bottom–bottom, and cross equalization (Santos et al. 2006). The same adsorbents, model and optimization logic were used as in the previous study. O_2 recovery was found to be higher and power consumption lower with equalization, with top-to-top equalization providing the best strategy. Oxysiv™ 7 resulted in the highest O_2 recovery (> 60%) and lowest power. Top–top equalization was also found to result in the smallest required product tank (bed/tank volume ratio ~ 3.6 for LiX). The performance of a commercial concentrator (Weinmann Oxymat 3) operating with a PSA cycle (P_H/P_L = 3.0 and Oxysiv™ 5), was compared with the modeling results. The total cycle time was 16 s (pressurization + production = 7 s and equalization down = 1 s, depressurization = 7 s and equalization up = 1 s). The length and diameter of adsorbent bed was 29.5 cm and 8 cm, respectively, while the tank length was 12.5 cm (diameter = 8 cm). An optimum O_2 recovery of ~ 32% was determined at an O_2 product flow rate of 4.3 lpm.

A multifactor optimization aimed at RPSA for POCs was performed by Zheng et al. (2017). The following five factors were selected for the optimization: dead zone heights (void volume) at the inlet and outlet of the adsorbent bed, pressurization and adsorption step times and the product extraction ratio, i.e. the fraction of the total O_2 exiting the bed that is retained as product, with balance used as purge. Four levels of each of these factors were considered in a modified design of experiments evaluation. This resulted in cycle times that varied from about 3.5 s to 17.5 s using a four-step Skarstrom type cycle. The adsorbent bed was 15 cm long and 5 cm diameter and contained 0.4 lb G5000 LiX (Arkema Ceca) having an average particle diameter of 1.6 mm. Momentum, material and energy balances were included in the model for an adiabatic bed with 2-D spatial coordinates. A porous media model of an axisymmetric bed was solved using CFD software. This computationally intensive simulation required one full day to complete ten PSA cycles. The five factor/four level analysis requiring 1024 simulations was necessarily reduced to 16 simulations by an orthogonal experimental design method. The cycle conditions included a constant air feed flow rate with P_H varying according to the pressurization time allowed. Relative importance of the five factors were evaluated with respect to BSF, O_2 purity, O_2 recovery and O_2 production rate. While quantitative results were obtained, the value of this study is probably more qualitative in view of the simplified cycle with no equalization, minimal thermal gradients, small number of cycles and undetermined kinetic effects. The complexity of the 2-D model would be better utilized by a 1-D model and more realistic operating conditions. Nevertheless, this study represents an important step toward meaningful optimization of complex cycles.

All three of the above studies ignore the presence of a pretreatment layer (thermal regenerator) and the former two ignore pressure drop and assume isothermal operation. These simplifications were likely included to save on the more intense computational demands of such optimization.

While not a process optimization in the same manner as the above studies, an interesting approach to minimizing weight of the POC establishes a relationship between PSA performance and the weight of three key components, i.e. compressor, battery and adsorbent (Dubois et al. 2003). Thus, design efficiency is measured in terms of the combined weight of these three components for 1.0 lpm of O_2 produced. Assuming the use of LiX (< 1 mm particles), cycle time of 15–20 s and O_2 recovery > 45% as conditions for optimum performance, the total specific weight (lb/lpm) of the three key components is suggested to be in the range of 1.4 to 8.8 lb/lpm. This can be compared to actual specific weights calculated in Table 3 for which all but one of the POCs is less than the upper limit "efficiency," noting that the total weight of the POCs includes all components. The lowest total specific weight in Table 3 (3.8 lb/lpm) suggests significant gains have been made by concentrator manufacturers in optimizing POCs since 2003.

An almost identical study was presented by Occhialini et al. (2009), except that the drive motor was not included in the weight of the compressor. The analysis was based upon a VPSA process that incorporated either four or five beds, rotating valves, 8-step or 10-step cycle (each with 1.0 s step times) and LiX (0.5 mm) adsorbent. The process was simulated (no details provided) for P_H = 1.2, 1.4 and 1.6 atm and a range of P_L from about 0.3 to 1 atm for 93% O_2 with product flows of 1.0, 2.0 and 3.0 lpm. The weight of each of the variable weight components (adsorbent, compressor and vacuum pump and battery) was estimated depending upon process operating conditions. The weight of the "fixed weight" components, including the compressor/pump drive motor, adsorbent enclosures, rotary valves and valve motor, product tank, electrical system, valves, POC case, etc., was unspecified. A minimum in the combined weight of the variable weight components was determined for a range of P_L for each of the process variables explored such that $0.75\ F_P < W_v < 2.02\ F_p$, i.e. for variable weight W_v in lb and product flow F_p in lpm. The absence of the motor weight makes it difficult to compare these results with those of Dubois et al. (2003).

5.3 MOC systems

The studies described above have been focused upon PSA or VPSA processes—both full and partial (individual steps in the cycle). POCs, in particular, are sophisticated systems that introduce operational variations and limitations to the process that typically do not exist in industrial scale air separation. Such variations and limitations include valve type and layout, compressor and pump types, bed design, pulse flow operation, cooling, case design, controls, FAA certification, weight and size, noise, etc. These features are typically addressed in the patent literature, although such features are often described without any direct reference to a detailed process description. It is notable that more than 150 patents were cited as prior art in a relatively recent POC patent (Deane and Taylor 2011). While important process patents have already been discussed above, only a sampling of the many apparatus patents will be summarized here.

A POC apparatus similar to the Caire Freestyle™ models in Table 3 is described by McCombs et al. (2004). This earlier version discloses a two-bed PSA/OCD combination capable of providing pulse doses from 8.75 ml to 43.75 ml. Each bed contains 81 g adsorbent. Air flow is nominally 7 lpm and a duration of 50 min is achieved for a fully charged battery. The improved version (McCombs et al. 2011) includes a custom two-headed compressor (McCombs et al. 2009) that can support either PSA or VPSA cycles with a nominal air flow rate of 6 lpm and a device weight < 5 lb. The unit operates with an 11 s cycle and three pulse settings.

A concentrator utilizing a six-step PSA cycle ($P_H = 35$ psia) that includes pressure equalization, feed/product pressurization overlap and purge with product is described by Deane et al. (2006). An O_2 recovery of 31–38% is claimed for an air flow rate varying between 4 and 9 lpm while producing an O_2 product rate ranging from 0.15 to 0.75 lpm. The apparatus weighs < 10 lb, utilizes a scroll compressor, Li-ion battery with 2 h rating and a conserver. The use of an adsorbent in the product tank is claimed to increase O_2 storage capacity. Pulse width modulation is added for improved valve actuation and compressor speed control (air flow rate control), which in turn provide for lower power and optimum battery utilization (Deane et al. 2010). An alternative free piston linear compressor is disclosed by Deane and Taylor (2011). A membrane dryer is added between the compressor and adsorber beds for the same O_2 concentrator (Taylor and Hansen 2010). Field replaceable adsorber beds allow smaller bed designs and address the issue of moisture contamination during shutdown and intermittent use (Taylor et al. 2017). Many of the features described in this paragraph appear to be consistent with the Inogen One® POCs of Table 3.

A POC system is described with emphasis on the controls for pulse flow O_2 delivery, valve actuation and compressor speed (Bliss et al. 2010). A detailed integrated description of the two-bed PSA process is not given, but the following preferences are independently stated: LiX adsorbent Oxysiv™ MDX (Honeywell UOP) in an amount of 1.0 lb/lpm O_2; $5 \leq P_H \leq 12$ psig; pretreatment layer for H_2O removal; 4-step cycle with about 12.4 s cycle time; control valves on feed side of beds and downstream of product reservoir; check valves and orifice between product end of beds and product reservoir. These parameters suggest a $P_H/P_L < 2.0$ and a relatively low O_2 recovery for the PSA process. It is claimed that the reciprocating, multi-head compressor may consume up to 95% of the overall device power, and that power may increase as much as 10% for each 1.0 psi increase in pressure drop. This patent is assigned to Respironics.

A dual mode O_2 generator is described wherein a detachable portable unit is coupled to a stationary base (Whitley et al. 2007). When detached, the POC unit operates with a production capacity of 0.5–3.0 lpm in either continuous or pulse flow mode. When coupled to the stationary base (which may contain a booster motor and pump), the device becomes a stationary MOC with production capacity of 0.5–5 lpm. Other unique features include a 5-bed concentrator utilizing a 10-step, 10 s VPSA cycle and rotary valves. A pretreatment layer and a LiX layer (0.25–1.0 mm particles) are disclosed along with $1.3 \text{ atm} \leq P_H \leq 2.5 \text{ atm}$ and $0.25 \text{ atm} \leq P_L \leq 0.65 \text{ atm}$. A portable-only unit was described with four beds and a rotary valve and scroll-type compressor/pump (Whitley et al. 2009). The POC operates with an 8-step VPSA cycle and may be designed for continuous and/or pulse flow modes for an O_2 production capacity of 0.5–3.5 lpm.

A wearable modular POC (utilizing VSA with feed, evacuation and re-pressurization steps) is described by Jagger et al. (2006). The device uses a positive displacement vacuum pump and a product control pump, wherein the latter is driven by vacuum from the vacuum pump. The feed step time is controlled by sensing the position of the MTZ, while the overall cycle time (0.5 to 5.6 s) is controlled according to the vacuum pump motor speed. The unit may be operated in either continuous or pulse flow mode to produce up to 1.5 lpm O_2 product using as little as 30 g LiX (Oxysiv™ MDX) dispersed within three beds. A POC weight less than 3.0 lb (including a battery weight less than 0.7 lb) is claimed for operation up to 4.0 h. If such performance were to be achieved, it would represent a significant improvement over all of the present commercial units described in Tables 3 and 5.

In all of the published studies and patents discussed in Sects. 5.2 and 5.3 above, as well as the manufacturers' published product information in Tables 1–5, there are essentially no specific air separation process operating conditions given for commercially available MOCs.

5.4 Alternative concepts

Conventional air separation processes are primarily characterized by one or two-bed, adsorber beds packed with spherical bead zeolites, operating with PSA, VPSA or VSA cycles comprising 4–12 steps and cycle times ranging from about 3–90 s. Alternative concepts include the use of multiple beds and rotary valves, structured adsorbents, high frequency cycles, etc. While most of these unconventional approaches have not met with wide commercial acceptance, they nevertheless represent important challenges to the paradigms of existing technologies. A few examples are given below.

Multiple beds ($\geq$ three beds) facilitate additional equalization steps and thereby promote higher O_2 recovery and lower power. Rotary valves are a common companion to the multi-bed approach for POCs and eliminate many individual valves in the system. An early system for stationary MOCs utilizes a rotary valve in combination with multiple bed and a variable speed compressor (Hill and Hill 1997). A POC system utilizing five beds and a rotary valve is described by Appel et al. (2004). Both of these inventions were assigned to SeQual Technologies, Inc. The latter discloses a nine-step VPSA cycle with two-up and two-down equalization steps, variable speed compressor and continuous O_2 product flow ranging from 1.0 slpm to 3.5 slpm. The experimental performance results are consistent with that achieved in industrial air separation, e.g. O_2 recovery of 45–71%, O_2 purity 86.3–94.5% for $2.5 \leq P_H/P_L \leq 3.5$, $1.5 \leq P_H \leq 1.8$ atm and $0.5 \leq P_L \leq 0.6$ atm. The variable speed compressor controls air flow rate from 7.0 to 26.9 slpm, while operating with an adiabatic compressor/pump power of 6.2 to 23.0 W/lpm O_2. No cycle times or adsorbent/bed specifications are linked directly to the experimental results. Several MOCs were commercialized by SeQual—only the Eclipse 5^{TM} (Caire, Inc.) is still available (see Table 5). It is unclear if this 18.4 lb combination POC incorporates the multi-bed/rotary valve technology. Some characteristics which may limit such technology in pulse flow-only POCs are the weight/size of additional beds and rotary valve, complexity of moving parts, the wear and sealing of valve surfaces and additional drive motor for the rotary valve.

An ultra-rapid cycle (yet another variation of RPSA terminology) with frequency > 1 cycle/s has been described by Galbraith et al. (2014a) for POCs. Key features include a two-bed PSA process containing 5–30 g molecular sieve (aluminophosphate or silica aluminophosphate exchanged with various optional cations). A replaceable module contains beds that are 2 cm diameter × 7 cm length, while adsorbent particle size ranges from 60 to 180 μm. The process is claimed to produce 0.75 to 1.0 lpm of 94% O_2 while achieving 33 to 36% O_2 recovery. This patent also describes an interesting moisture management system that consists of two coaxial vessels with the inner cylinder of each vessel containing a moisture adsorbing or getter material. This core cylinder is separated from the annulus by a moisture permeable (but gas impermeable) barrier. Air flows through the two annuli in series while product O_2 flows through the core of one vessel and waste N_2 flows through the core of the other vessel. Moisture diffuses from the air through the barrier and into the core material. Product O_2 is rehydrated as it passes through the one core and on to the patient, while relatively dry waste N_2 picks up moisture as it flows through the other core.

An extension of the above technology is directed at oxygen enriched air (OEA) where there is created the options of continuous or pulse flow of high purity O_2 ($\geq$ 90%) or continuous flow of OEA containing from 30 to 90% O_2 (Galbraith et al. 2014b). The example device weighs 1.0 lb or less and has the following characteristics: 5 g LiX (80–140 μm) in a single bed (12 mm dia. × 80 mm length), air flow 1.5 – 2.5 lpm, P_H = 180 kPa, cycle time of 1.6 s to 3.3 s, 400 ml/min OEA at 32% O_2 or 30 – 40 ml/min of 90% O_2.

A high frequency process (10 cycles/s) utilizing piston driven compression and evacuation at each end of a single bed is presented as a means to minimize energy loses and maximize the ratio of product volume to energy consumed (Jagger et al. 2003). Pressurization, gas shift and depressurization represent the three steps in the process, with product O_2 withdrawn during the gas shift step.

Structured adsorbents are frequently suggested in various patents as low ΔP, low mass transfer resistance and high throughput alternatives to packed beds. An informative investigation comparing monoliths, laminates and foams to packed beds containing beaded adsorbents was performed for the example separation of 10% CO_2 from N_2 using NaX (Rezaei and Webley 2009). Key structural parameters identified included adsorbent density, ΔP/unit length, total void volume, external surface area/unit volume and dispersion. The mass transfer mechanism differs between the structured materials and with beads. Laminate structures with thin walls and small spacing (< 0.2 mm) showed promise for high throughput (inverse of BSF) when faster cycles and higher superficial velocities are desirable. Monoliths are limited by the current lower practical cell densities. The review did not address the difficulties in manufacturing, drying/calcination and handling of

structured zeolite materials. Additionally, air separation represents one of the more challenging applications for structured materials due to the high adsorbent density required.

A rotary PSA or VPSA module containing three adsorber modules has been described for high frequency operation in MOCs (Keefer et al. 2007). The adsorbent is impregnated or otherwise supported on a thin (100–170 μm) inert laminate sheet or sheets and loaded into each module in layers or as a spirally wound body with channels formed between layers by separators in both configurations. Various cycle step options are presented, but operating conditions and performance are not provided.

A process similar to the high ΔP RPSA cycles described in Sect. 5.2.1 above was combined with a "monolithic adsorbent bed" in a modeling study (Kopaygorodsky et al. 2004). The bed measured 20 mm in diameter, was 2 mm thick and contained 2 μm diameter particles of 5A zeolite—a particle size typical of zeolite powder. However, this configuration appears to be better described as a laminate structure. A two-step process included pressurization and depressurization with nominal step times of 1 s and 2 s, respectively. The model was formulated with dimensionless variables and solved to determine 85% O_2 purity, 56% O_2 recovery and a BSF = 14 lb/TPDO. There was no information regarding how such an adsorbent structure might be produced.

An adsorbent e.g. Oxysiv^{TM} 5 is combined with a polymer to create an immobilized adsorbent that can be shaped and/or fit into a fixed container (Gaita et al. 2003). Further processing such as leaching the majority of the polymer, drying, etc. are performed to result in a porous bound structure that essentially retains all of it adsorption capacity.

A concentrator is combined with a liquefier and storage device to produce both gaseous O_2 and LOX (Boissin and Hennebel 2001). An example would be a stationary concentrator operating with excess O_2 capacity such that some of the excess O_2 is diverted to a liquefier to produce LOX to be stored in a removable ambulatory container that could be used to increase mobility of the patient.

6 Challenges to further improvements to MOCs

The current state-of-the-art of MOCs is best viewed from the operating characteristics given in Tables 1 and 3 for stationary and portable devices, respectively. There is a factor of three difference in weight (power also varies from 275 to 385 W) for the commercial stationary concentrators listed in Table 1, i.e. there remains little difference in the other performance characteristics. This disparity in weight and power suggests possible differences in compressor, adsorbent, and/or air separation technologies. It should be relatively straight forward to apply the intensification strategies summarized in Sects. 4 and 5 (along with some considerations of improved adsorbents, smaller particle size and reduced BSF from Sect. 5) to reduce the weight and improve process efficiency of the heaviest concentrators. With the market shifting toward POCs, there may be little incentive for some manufactures to improve their stationary concentrator offerings – particularly in view of the relatively low price of these devices and the likely high investment cost required for redesign and retooling of the enclosure and components.

The characteristics of the POCs listed in Table 3 were discussed in Sect. 3 and it is apparent that there are significant differences in performance (weight, O_2 capacity and duration) amongst these devices. POCs are sophisticated systems that have been improved significantly since their inception nearly two decades ago. Differentiating these devices on the basis of technology employed is challenging without greater exposure of the key components and processes utilized. As noted above, the state-of-the-art of POCs with respect to adsorption technology is difficult to assess due the lack of process operating details for the devices. The total device specific weight (lb/lpm) compared in Table 3 differs by more than a factor of two for the various manufacturers. This suggests that the technology of some POCs is more advanced than that of others.

Utilizing the information collected in this review and inferring the state of the air separation technology employed in POCs, potential improvements and areas for future study have been identified and are offered below.

6.1 Adsorbents

In the past three decades since Chao (1989) introduced LiX (Si/Al = 1.0) there have been no serious rivals to displace this adsorbent for air separation. Of course LiX has also been continuously improved over this period. The state-of-the-art in LiX technology can be summarized as follows:

- Si/Al = 1.0
- Li content $\geq$ 98%
- Binder content $\leq$ 10%
- Binder Type: various clay and non-clay
- Improved pore morphology for high rate

These characteristics apply to adsorbents for both industrial scale and concentrator applications. Smaller particle diameters (average diameter 0.4–0.6 mm) are offered for concentrators. Although not all of these attributes may be found in each of the commercial LiX adsorbents in Table 7 above, the available materials are

generally durable and of high quality. While incremental improvements to LiX are likely to continue, this material's development is mature. Because advanced adsorbents are a "drop-in" improvement to concentrators, it is likely that many of the current devices are utilizing the materials included in Tables 6 and 7 of Sect. 5.1. Nevertheless, this does not guarantee that the concentrator processes are taking full advantage of the performance that these adsorbents offer.

Adsorbent research continues to be very active for many different gas separations. The commercial importance of air separation will motivate searches for better materials, although separation performance is only part of the challenge. Developing cost effective manufacturing methods and creating adsorbents suitable for use in fixed beds or as structured materials are longer term pursuits.

6.2 Processes

Improvements in compressors and batteries can be immediately implemented with benefits accruing to lower power consumption, reduced weight and/or longer duration. The focus here is upon increased air separation process efficiency (BSF, O_2 recovery, product capacity and unit power). In reviewing the progress in air separation process technology (as reflected primarily in the published literature authored from the adsorption community), and in particular as it relates to the application in MOCs, it is apparent that the perspective has been predominantly one of continuous flow, i.e. the same as in industrial air separation. As a result, some of the unique characteristics of pulse flow devices have been overlooked in pursuit of faster cycles, smaller particles and lower BSF. Nevertheless, it is instructive to establish a level of the advanced state of air separation process performance as it relates to concentrators, albeit with the inherent assumption that it was born out of continuous flow processes.

The intensification studies (following Wankat's scaling rules) cited above provide demonstrated performance for fast cycle air separation processes as follows:

- Total cycle time: $\leq$ 5 s
- Adsorbent: LiX (Si/Al = 1.0)
- Particle size: $\approx$ 0.4 mm – 0.6 mm
- BSF $\leq$ 50 lb/TPDO (0.11 lb/lpm)
- O_2 recovery:

  VPSA: 40–60%
  PSA: 35–50%

- Unit power (power per unit of O_2 produced):

  VPSA: $\leq$ 56.5 W/lpm (25 kW/TPDO)
  PSA: $\leq$ 67.8 W/lpm (30 kW/TPDO)

These results also reflect 6–8 cycle process steps, including equalization, product pressurization and purge with product (also using commercial improved rate and prototype high rate adsorbents). These characteristics and performance simply serve as an approximate benchmark for further discussion.

The RPSA studies summarized in Sect. 5.2.3 concentrated primarily on defining limits in cycle time, particle size and BSF. They offered insight for problems arising from very short cycles and small particles. Results were varied and broadened with respect to the performance parameters listed above. The fact that many of these studies ignored power, thermal effects, bed ΔP and pressure limitations make it difficult to draw conclusions that can be practically applied in POC design. This is further exacerbated by O_2 recovery often obtained well below what is expected and demonstrated from industrial air separation and intensified MOC studies.

6.2.1 Unique operating characteristics of POCs

The inherent advantage of pulse flow operation is the ability to produce O_2 in a demand mode that meet the O_2 saturation requirements of the patient. This is accomplished through a series of pulse settings, i.e. with increasing air flow and a corresponding increase in the amount of O_2 at each higher pulse setting. This is implemented operationally by controlling the speed of the compressor motor, which in turn reduces power consumption and increases concentrator operation time. It is recognized that the concentrator still functions in continuous flow at all pulse settings. However, designing the concentrator (fixed bed design) so that it can operate at several distinctly different air flow rates and peak pressures is a marked departure from the typical operation of industrial air separation processes – although a single turn-down condition is occasionally used for short durations in the larger systems.

Opportunities for future challenging studies are suggested as follows:

1) The lower compressor motor speeds (at lower pulse settings) correspond to lower air flow rates, potentially lower peak pressure and/or longer time to reach peak pressure. This may necessitate the adjustment of the cycle step times to maintain desired O_2 product purity. Summarizing, each pulse setting represents a different operating condition in terms of one or more of the following parameters: air flow, cycle time, peak pressure and P_H/P_L– all for the same fixed bed design. Clearly, optimal equalization, purging and product pressurization requirements would differ for each pulse setting. This operational departure from industrial air separation processes presents many

interesting questions – few, if any, have been addressed in the adsorption literature. There is substantial opportunity to study these various conditions in an effort to determine the best slate of parameters across the pulse setting range to maximize O_2 production and minimize power and weight.

Furthermore, it is possible that intensification to the shortest cycle time and lowest BSF is not the best strategy to support the varied operational conditions of pulse flow. More time may be required for pressurization, purging, etc. at the lower pulse settings. Intensification to achieve a specific weight of 0.1 to 0.5 lb/lpm offers a potential range of cycle times from about 5 s to 20 s. Even as much as 0.5 lb adsorbent represents less than 10% of the overall weight of most of the POC devices in Table 3.

2) While both PSA and VPSA processes have been implemented in POCs, the use of PSA seems to be preferred. While VPSA offers the potential for higher O_2 recovery, the combination of compressor/vacuum pump heads driven by a single motor may represent greater weight and possibly greater power, e.g. compressor models 2250z vs. 2220z (Gardner Denver Thomas 2019c). Evacuation with purge offers the potential to improve desorption of H_2O and CO_2 from the pretreatment layer, but the vacuum condition at the start of pressurization may impact the time to reach peak pressure. Both PSA and VPSA options need to be better understood under the varying operating conditions of pulse flow devices as indicated in 1) above. It appears that the small compressors/pumps can be customized for specific sets of process conditions with potential to optimize for both low power and weight.
3) The relatively low O_2 recoveries obtained in most of the studies reviewed in Sect. 5.2.3 are puzzling. Likewise, the limited process performance information for POCs suggest lower recovery than could be potentially achieved. Whether this is the inherent in the varied operating conditions or simply due to non-optimized process cycles is unclear. Higher O_2 recovery can be utilized to achieve lower BSF, reduced compressor air flow rate and compressor weight, longer duration and/or lower power. Thus, there are large incentives to maximizing O_2 recovery.
4) Sizing the pretreatment layer in fast cycle processes has been given little attention. Due to the strong affinity of H_2O by NaX, a large residual loading of H_2O prevails in PSA and VPSA cycles. The residual is considerably larger than the amount of H_2O entering the layer during each cycle. The pretreatment layer can be completely characterized as MTZ. As such, the intensification strategies that rely on the motion of a constant pattern mass transfer front do not apply. If the layer is not properly sized, then water enters the LiX layer and effectively reduces the useable bed depth. Studying this problem is further complicated by the refrigeration and thermal regenerative effects resulting from the combination of the two layers. Mass transfer rate effects may also be important under these conditions.

A second potential problem is the diffusion of H_2O and/or CO_2 from the pretreatment layer (or from ambient air) into the N_2-selective layer when the POC is not in operation. This condition has been acknowledged in fast cycle, intermittent use POCs as responsible for the shorter life of the adsorber beds (Babicki et al. 2006; Taylor and Hansen 2010; Taylor et al. 2017). While various methods of mitigation have been employed, a better understanding of the diffusive mechanisms is needed.

Other drying technologies to replace or supplement the pretreatment layer may represent opportunities for improved moisture and CO_2 removal, e.g. Galbraith et al. 2014b; Taylor and Hansen 2010.

6.3 Experiments and modeling

Section 4 of this review was included to not only summarize the progress in air separation technology, but also to bring attention to the important elements needed to successfully model and test such processes. Simplifying assumptions can be appropriate for evaluating new complex processes. The well-developed maturity of air separation processes affords no such luxury. Ignoring important features such as the pretreatment layer, pressure drop, thermal effects and using compressed air in place of a representative compressor/pump significantly impact the quality and practical relevance of the results from both experiments and simulations.

Including H_2O and CO_2 can greatly complicate both modeling and experiments. However, the use of an inert layer of similar heat capacity and particle size captures the majority of the thermal regenerative effects of the pretreatment layer (Wilson et al. 2001). The small beds of MOCs are not isothermal, even with the high wall surface area to adsorbent volume ratio. The mass transfer rates are significantly higher than the heat transfer rates such that heat dissipation is too slow to achieve isothermal operation.

MOC processes may be experimentally investigated in the laboratory at full scale – unlike industrial scale air separation processes. Representative valves, compressors, vacuum pumps, product tanks, adsorber beds, etc. can and should be used. It is particularly important to incorporate compressors/pumps, e.g. those offered by Gardner Denver Thomas or from POC manufacturers. This insures that

realistic pressurization, pressure drop and power consumption effects are automatically included in the performance results. Studies that do not include power ignore one of the most important performance factors for POCs.

Cyclic steady state should be determined on the basis of temperature changes over multiple cycles. Attention should also be given to inlet/outlet voids, dense packing of the bed, and measurement of isotherms and mass transfer coefficients for the particular adsorbent(s) used in the evaluation. It is also necessary to ensure that the initial condition of adsorbents is fully activated with no H_2O contamination. While attending to all of these concerns can be tedious and time-consuming, the effort is justified in the quality of the results achieved. Finally, further POC development could be greatly facilitated by a closer collaboration between MOC manufacturers and the adsorption community.

7 Conclusions

Air separation is one of a number of important cyclic adsorptive processes. Significant innovations in both adsorbents and processes have enabled widespread commercialization of this technology. This review presents important steps in the evolution of this technology as it applies to both industrial and MOC systems. Adsorbent and process development have been largely driven by industrial air separation, but the advances in this technology were quickly adopted to create an important alternative to compressed gas and LOX used in LTOT. While early MOCs were large stationary units designed for home use, the introduction of OCD and pulse flow are rapidly changing the market for these devices. POCs offer greater mobility options for LTOT patients in addition to air travel.

LiX adsorbents, superior for air separation, have been continuously developed and extended with small particle options for MOCs. With the exception of some differences related to the scale of equipment components, stationary MOC processes are generally smaller versions of their industrial scale relatives. Conversely, POCs introduce operational differences that impact both the design and conditions of the adsorption process. Some of these differences have been overlooked in adsorption studies and consequently offer opportunities for expanded understanding of non-conventional process operating characteristics. These opportunities have been identified and hopefully can be exploited to further improve efficiency (weight, power, duration and O_2 product capacity) of future POCs.

Acknowledgements The author is grateful for informative discussions with the following individuals: S. De Noia (Honeywell UOP), G. Halsinger (Gardner Denver Thomas), P. Hansen (Inogen), K. Knaebel (Adsorption Research, Inc.), B. Meyers (Inogen), B. Taylor (Inogen), and K. Weston (Zeochem®). Thanks also goes to C. Barnes (Caire, Inc.), O. Philardeau (Arkema Ceca), and R. Lee (Jalon) for providing useful product information. Constructive comments on this manuscript from P. Barrett, A. Moran and N. Stephenson (all from Linde PLC) are greatly appreciated.

References

Ackley, M.W.: Multilayer adsorbent beds for PSA gas separation. US Patent 6,152,991 (2000)

Ackley, M.W., Leavitt, F.W.: Rate-enhanced gas separation. US Patent 6,500,234 B1 (2002)

Ackley, M.W.: Adsorptive separation performance improvements resulting from enhanced adsorption rate. 225th ACS National Meeting, New Orleans (2003a)

Ackley, M.W., Rege, S.U., Saxena, S.: Application of natural zeolites in the purification and separation of gases. Microporous Mesoporous Mater. **61**, 25–42 (2003b)

Ackley, M.W., Smolarek, J., Leavitt, F.W.: Pressure swing adsorption gas separation method, using adsorbents with high intrinsic diffusivity and low pressure ratios. US Patent 6,506,234 B1 (2003c)

Ackley, M.W., Zhong, G.: Medical oxygen concentrator. US Patent 6,551,384 B1 (2003d)

Ackley, M.W., Barrett, P.A.: Silver-exchanged zeolites and methods of manufacturing therefor. US Patent 7,455,718 B2 (2008).

Ackley, M.W., Barrett, P.A., Stephenson, N.A., Kikkinides, E.S.: High rate compositions. US Patent 9,533,280 B2 (2017)

Air Squared, Inc.: https://airsquared.com/custom-design/project-portfolio/compact-oil-free-scroll-compressor-medical-devices/, Accessed 26 Apr 2019

Alpay, E., Kenney, C.N., Scott, D.M.: Adsorbent particle size effects in the separation of air by rapid pressure swing adsorption. Chem. Eng. Sci. **49**, 3059–3075 (1994)

Appel, W.S., Winter, D.P., Sward, B.K., Sugano, M., Salter, E., Bixby, J.A.: Portable oxygen concentration system and method of using the same. US Patent 6,691,702 (2004)

Armond, J.W., Webber, D.A.: Adsorption system. US Patent 3,923,477 (1975)

Babicki, M.L., Keefer, B.G., Gibbs, A.C., LaCava, A.I., Fitch, F.: PSA with adsorbents sensitive to contaminants. US Patent 7,037,358 B2 (2006)

Baksh, M.S.A., Kikkinides, E.S., Yang, R.T.: Lithium type X zeolite as a superior sorbent for air separation. Sep. Sci. Technol. **27**, 277–294 (1992)

Baksh, M.S.A., Kibler, V. J., Schaub, H.R.: Pressure swing adsorption process. US Patent 5,518,526 (1996)

Batta, L.B.: Selective adsorption gas separation process. US Patent 3,636,679 (1972)

Barrett, P.A., Pontonio, S.J., Kechagia, P., Stephenson, N.A., Weston, K.C.: Adsorbent composition. US Patent 9,050,582 B2 (2015)

Berlin, N.H.: Method for providing oxygen-enriched environment. US Patent 3,280,536 (1966)

Berlin, N.H.: Vacuum cycle adsorption. US Patent 3,313,091 (1967)

Bird, R.B., Stewart, W.E., Lightfoot, E.N.: Transport phenomena. Wiley, New York (1960)

Bliss, P.L., McCoy, R.W., Adams, A.B.: A bench study comparison of demand oxygen delivery systems and continuous flow oxygen. Respir. Care **44**, 925–931 (1999)

Bliss, P.L., Atlas, C.R., Halperin, S.C.: Portable oxygen concentrator. US Patent 7,837,761 B2 (2010)

Boissin, J.C., Hennebel, V.: Portable home oxygen therapy medical equipment. US Patent 6,314,957 B1 (2001)
Breck, D.W.: Zeolite molecular sieves: structure, chemistry and use. Wiley, New York (1974)
Campbell, M.J., Lagree, D.A., Smolarek, J.: Advances in oxygen production, by pressure swing adsorption. In: Gaden, E.L., Wenzel, L.A. (eds.), Cryogenic Processes and Machinery. AIChE Symposium Series vol 89, no. 294, pp. 104–108, AIChE, New York (1993)
Carlin, B.W., McCoy, R., Diesem, R.: 2 is not 2 is not 2, the fundamental flaw in perception when providing long-term oxygen therapy (LTOT) to a patient. Respir. Ther. **13**, 29–32 (2018)
Cassidy, R.T., Holmes, E.S.: Twenty-five years of progress in "adiabatic" adsorption processes. AIChE Symp. Ser. 80 (No. 233), 68–75 (1984)
Celik, C.E., Ackley, M.W., Smolarek, J.: Modular compact adsorption bed. US Patent 8,268,043 B2 (2012)
Chai, S.W., Kothare, M.V., Sircar, S.: Rapid pressure swing adsorption for reduction of bed size factor of a medical oxygen concentrator. Ind. Eng. Chem. Res. **50**, 8703–8710 (2011)
Chai, S.W., Kothare, M.V., Sircar, S.: Numerical study of nitrogen desorption by rapid oxygen purge for a medical oxygen concentrator. Adsorption **18**, 87–102 (2012)
Chai, S.W., Kothare, M.V., Sircar, S.: Efficiency of nitrogen desorption from Lix zeolite by rapid oxygen purge in a pancake adsorber. AIChE J. **59**, 365–368 (2013)
Chatburn, R.L., Lewarski, J.S., McCoy, R.W.: Nocturnal oxygenation using a pulsed-dose oxygen-conserving device compared to continuous flow. Respir. Care **51**, 252–256 (2006)
Chatburn, R.L., Williams, T.J.: Performance comparison of 4 portable oxygen concentrators. Respir. Care **55**, 433–442 (2010)
Chatburn, R.L., Williams, T.J.: Comparison of four under 5 lb. Portable oxygen concentrators. Strategic Dynamics, Inc. White Paper (March 7, 2013). https://inogen.com/pdf/White_Paper_Under_5_lb_POC5_03_07_13.pdf. Accessed 4 Jan 2019
Chao, C.C.: Process for separating nitrogen from mixtures thereof with less polar substances. US Patent 4,859,217 (1989)
Chao, C.C., Pontonio, S.J.: Advanced adsorbent for PSA. US Patent 6,425,940 B1 (2002)
Coe, C.G., S.M. Kuznicki: Polyvalent ion exchanged adsorbent for air separation. US Patent 4,481,018 (1984)
Collins, J.J.: The LUB/equilibrium section concept for fixed-bed adsorption. Chem. Eng. Prog. Symp. Ser. **63**(74), 31–35 (1967)
Collins, J.J.: Air separation by adsorption. US Patent 4,026,680 (1977)
Cotes, J.E., Douglas-Jones, A.G., Saunders, M.J.: A 60% oxygen supply for medical use. Br. Med. J. **4**, 143–146 (1969)
Cruz, P., Santos, J.C., Magalhães, F.D., Mendes, A.: Cyclic adsorption separation processes: analysis strategy and optimization procedure. Chem. Eng. Sci. **58**, 3143–3158 (2003)
Dangieri, T. J., Cassidy, R.T.: RPSA process. US Patent 4,406,675 (1983)
Deane, G.F., Taylor, B.A., Bare, R.O., Scherer, A.J.: Portable gas fractionalization system. US Patent 7,066,985 B2 (2006)
Deane, G.F., Taylor, B.A., Li, C.M.: Portable gas fractionalization system. US Patent 7,753,996 B1 (2010)
Deane, G.F., Taylor, B.A.: Portable gas fractionalization system. US Patent 7,922,789 B1 (2011)
de Klerk, A.: Voidage variation in packed beds at small column to particle diameter ratio. AIChE J. **49**, 2022–2029 (2003)
Dubois, A., Bodelin, P., Vigor, X.: Portable oxygen concentrator. US Patent 6,520,176 B1 (2003)
Dunne, P.J.: The clinical impact of new long-term oxygen therapy technology. Respir. Care **54**, 1100–1111 (2009)
Earls, D.E., Long, G.N.: Multiple bed rapid pressure swing adsorption for oxygen. US Patent 4,194,891 (1980)
Ergun. S.: Fluid flow through packed columns. Chem. Eng. Prog. **48**, 89–94 (1952)
Federal Aviation Authority (FAA): Acceptance criteria for portable oxygen concentrators used on board aircraft; final rule. Fed. Register **81**(100), 33098–33122 (2016)
Gaffney, T.R.: Porous solids for air separation. Curr. Opin. Solid State Mater. Sci. **1**, 69–75 (1996)
Gaita, R., Yates, S.F., Zhou, S.J., Chang, C.H.: Polymer-bound nitrogen adsorbent. US Patent 6,585,810 B1 (2003)
Galbraith, S.D., McGowan, K.J., Baldauff, E.A., Galbraith, E., Walker, D.K., LaCount, R.B.: Ultra rapid cycle portable oxygen concentrator. US Patent 8,894,751 B2 (2014a)
Galbraith, S.D., Walker, D.K., McGowan, K.J., DePetris, E.N., Galbraith, J.C.: Portable oxygen enrichment device and method of use. US Patent 8,888,902 B2 (2014b)
Gardner Denver Thomas Web: https://www.gd-thomas.com (2019a). Accessed 11 Jan 2019
Gardner Denver Thomas Web: https://www.gd-thomas.com/en/media/catalog/gdt_brochure/2250Z_WOB-L_4011_06_17_1.pdf (2019b). Accessed 11 Jan 2019
Gardner Denver Thomas Web: https://www.gd-thomas.com/en/media/catalog/gdt_brochure/2220Z_WOB-L_4005_09_17_1.pdf (2019c). Accessed 11 Jan 2019
German, R.M.: Particle packing characteristics. Metal Powder Industries Federation, Princeton (1999)
Goshorn, J.C., Gross, W.E.: Volume meter for granular materials. US Patent 2,332,512 (1943)
Gross, W.E.: Packing granular materials. Mech. Eng. **84**, 469–472 (1949)
Guerin De Montgareuil, P., Domine, D.: Process for separating a binary gaseous mixture by adsorption. US Patent 3,155,468 (1964)
Hay, L., Vigor, X.: Adsorber and process for the separation by adsorption. US Patent 5,176,721 (1993)
Hill, C.C., Hill, T.B.: Fluid fractionator. US Patent 5,593,478 (1997)
Hirano, S., Kawamoto, T., Nishimura, T., Yoshimura, K.: Adsorbent for separating gases. US Patent 6,171,370 B1 (2001)
Hirooka, E., Wheatland, J.P., Doong, S.J.: Process for producing oxygen enriched product stream. US Patent 5,122,164 (1992)
Hu, X., Mangano, E., Friedrich, D., Ahn, H., Brandani, S.: Diffusion mechanism of CO_2 in 13X zeolite beads. Adsorption **20**, 121–135 (2014)
Izumi, J.: High Efficiency oxygen separation with low temperature and low pressure PSA. AIChE San Francisco, Nov. 1989
Jacobs, S.S., Lederer, D.J., Garvey, C.M., Hernandez, C., Lindell, K.O., McLaughlin, S., Schneidman, A.M., Casaburi, R., Chang, V., Cosgrove, G.P., Devitt, L., Erickson, K.L., Ewart, G.W., Giordano. S.P., Harbaugh, M., Kallstrom, T.J., Kroner, K., Krishnan, J.A., Lamberti, J.P., Porte, P., Prieto-Centurion, V., Sherman, S.E., Sullivan, J.L., Sward, E., Swigris, J.J., Upson, D.J.: Optimizing home oxygen therapy, An Official American Thoracic Society Workshop Report. Ann. Am. Thorac. Soc. **15**, 1369–1381 (2018)
Jagger, T.W., Van Brunt, A.E., Van Brunt, N.P.: Pressure swing adsorption gas separation method and apparatus. US Patent 6,641,644 B2 (2003)
Jagger, T.W., Van Brunt, N.P., Kivisto, J.K., Lonnes, P.B.: Portable oxygen concentrator. US Patent 7,121,276 B2 (2006)
Jee, J.G., Lee, J.S., Lee, C.H.: Air separation by a small-scale two-bed medical O_2 pressure swing adsorption. Ind. Eng. Chem. Res. **40**, 3647–3658 (2001)
Jones, R.L., Keller II, G.E., Wells, R.C.: Rapid pressure swing adsorption process with high enrichment factor. US Patent 4,194,892 (1980)

Kaplan, R.H., Dunne, S.R., McKeon, M.J.: Advances in the design of medical oxygen concentrators. AIChE Meeting, San Francisco, 1–6, (1989)
Keefer, B.G., McLean, C.R., Babicki, M.L.: Life support oxygen concentrator. US Patent 7,250,073 B2 (2007)
Kenyon, F.D., Puckhaber, J.W.: Flow controller. US Patent 4,784,130 (1988)
Kikkinides, E.S., Politis, M.G.: Linking pore diffusivity with macropore structure of zeolite adsorbents. Part I: three dimensional structural representation combining scanning electron microscopy with stochastic reconstruction methods. Adsorption **20**, 5–20 (2014a)
Kikkinides, E.S., Politis, M.G.: Linking pore diffusivity with macropore structure of zeolite adsorbents. Part II: simulation of pore diffusion and mercury intrusion in stochastically reconstructed zeolite adsorbents. Adsorption **20**, 21–35 (2014b)
Knaebel, K.S., Kandybin, A.: Pressure swing adsorption system to purify oxygen. US Patent 5,226,933 (1993)
Kopaygorodsky, E.M., Guliants, V.V., Krantz, W.B.: Predictive dynamic model of single-stage ultra-rapid pressure swing adsorption. AIChE J **50**, 953–962 (2004)
Kratz, W.C., Sircar, S.: Pressure swing adsorption process for medical oxygen generator for home use. US Patent 4,477,264 (1984)
Kulish, S., Swank, R.P.: Rapid cycle pressure swing adsorption oxygen concentration method and apparatus. US Patent 5,827,358 (1998)
Kumar, R.: Vacuum swing adsorption process for oxygen production—a historical perspective. Sep. Sci. Technol. **31**, 877–893 (1996)
Kuznicki, S.M., Coe, C.G., Jenkins, R.J., Butter, S.A.: Massive bodies of maximum aluminum X-type zeolite. US Patent 4,606,040, (1986)
Langer, G., Roethe, A., Roethe, K.-P., Gelbin, D.: Heat and mass transfer in packed beds-III. Axial mass dispersion. Int. J. Heat Mass Transfer 21, 751–759 (1978)
LaSala, K.A., Schaub, H.R.: Single bed pressure swing adsorption system and process. US Patent 5,370,728 (1994)
Leavitt, F.W.: Air separation pressure swing adsorption process. US Patent 5,074,892 (1991)
Leavitt, F.W.: Low temperature pressure swing adsorption with refrigeration. US Patent 5,169,413 (1992)
Leavitt, F.W.: Lithium recovery. US Patent 5,451,383 (1995)
Leavitt, F.W.: Thermally-driven ion-exchange process for lithium recovery. US Patent 5,681,477 (1997)
LeBlanc, C.J., Lavallee, L.G., King, J.A., Taylor-Sussex, R.E., Woolnough, A., McKim, D.A.: A comparative study of 3 portable oxygen concentrators during a 6-minute walk test in patients with chronic lung disease. Respir Care **58**, 1598–1605 (2013)
Lu, Z., Rodrigues, A.E.: Intensification of sorption processes using "large-pore" materials. Ind. Eng. Chem. Res. **32**, 230–235 (1993)
Lu, Z.P., Loureiro, J.M., LeVan, M.D., Rodrigues, A.E.: Intraparticle diffusion/convection models for pressurization and blowdown of adsorption beds with langmuir isotherm. Sep. Sci. Technol. **27**, 1857–1874 (1992)
Lukchis, G.M.: Adsorption systems part I: design by mass-transfer-zone concept. Chem. Eng., 111–116 (1973)
Maring, B.J., Webley, P.A.: A new simplified pressure/vacuum swing adsorption model for rapid adsorbent screening for CO_2 capture applications. Inter. J. Greenh. Gas Control **15**, 16–31 (2013)
Martin, H.: Low peclet number particle-to-fluid heat and mass transfer in packed beds. Chem. Eng. Sci. **33**, 913–919 (1978)
McCombs, N.R.: Selective adsorption gas separation process. US Patent 3,738,087 (1973)
McCombs, N.R.: Compact oxygen concentrator. US Patent 4,378,982 (1983a)
McCombs, N.R.: Bed vessels for compact oxygen concentrator. US Patent 4,371,384 (1983b)
McCombs, N.R.: Portable low profile dc oxygen concentrator. US Patent 4,826,510 (1989)
McCombs, N.R.: Compact compressor. US Patent 7,491,040 B2 (2009)
McCombs, N.R., Schlaechter, J.: Compact oxygen concentrator. US Patent 4,302,224 (1981)
McCombs, N.R., Schlaechter, J.: Compact oxygen concentrator. US Patent 4,342,573 (1982)
McCombs, N.R., Casey, R.E., Chimiak, M.A., Klimaszewski, A.: Portable oxygen concentrator. US Patent 6,764,534 (2004)
McCombs, N.R., Bosinski, R., Casey, R.E., Valvo, M.R.: Mini-portable oxygen concentrator. US Patent 8,016,925 (2011)
McCoy, R.W.: Oxygen-conserving techniques and devices. Respir Care **45**, 95–103 (2000)
McCoy, R.W.: Options for home oxygen therapy equipment: storage and metering of oxygen in the home. Respir. Care **58**, 65–85 (2013)
McCoy, R.W., Diesem, R.: Performance variability identified by bench testing of selected portable oxygen concentrators. Valley Inspired Products Inc. (August 23, 2018) https://www.gcehealthcare.com/wp-content/uploads/2018/08/Zen-o-lite-and-three-other-POCs-comparison-whitepaper-2018.pdf. Accessed 15 Dec 2018
Miller, G.Q.: Multiple zone adsorption process. US Patent 4,964,888 (1990)
Milton, R.M.: Molecular sieve adsorbents. US Patent 2,882,244 (1959)
Moran, A., Talu, O.: Role of pressure drop on rapid pressure swing adsorption performance. Ind. Eng. Chem. Res. **56**, 5715–5723 (2017)
Moran, A., Patel, M., Talu, O.: Axial dispersion effects with small diameter adsorbent particles. Adsorption **24**, 333–344 (2018a)
Moran, A., Talu, O.: Limitations of portable pressure swing adsorption processes for air separation. Ind. Eng. Chem. Res. **57**, 11981–11987 (2018b)
Moreau, S., Barbe, C.: Process for the separation of mixtures of oxygen and of nitrogen employing an adsorbent with improved porosity. US Patent 5,672,195 (1997)
Notaro, F., Mullhaupt, J.T., Leavitt, F.W., Ackley, M.W.: Adsorption process and system using multilayer adsorbent beds. US Patent 5,674,311 (1997)
Nowobilski, J.J., J. S. Schneider: Particle loader. US Patent 5,324,159 (1994)
Occhialini, J.M., Whitley, R.D., Wagner, G.P., LaBuda, M.J., Steigerwalt, C.E.: Weight-optimized portable oxygen concentrator. US Patent 7,473,299 B2 (2009)
Park, Y., Moon, D.K., Kim, Y.H., Ahn, H., Lee, C.H.: Adsorption isotherms of CO_2, CO, N_2, CH_4, Ar, H_2 on activated carbon and zeolite LiX up to 1.0 MPa. Adsorption **20**, 631–647 (2014)
Peterson, D.: Influence of presorbed water on the sorption of nitrogen by zeolites at ambient temperatures. Zeolites **1**, 105–112 (1981)
Petty, T.L.: Historical highlights of long-term oxygen therapy. Respir Care **45**, 29–36 (2000)
Plee, D.: Method for obtaining LSX zeolite bodies. US Patent 6,264,881 B1 (2001)
Plee, D.: Agglomerated adsorbent, process for the production thereof and use thereof for the non-cryogenic separation of industrial gases. US Patent 6,652,626 B1 (2003)
Pritchard, C.L., Simpson, G.K.: Design of an oxygen concentrator using rapid pressure-swing adsorption principle. Chem. Eng. Res. Des. **64**, 467–471 (1986)

Rama Rao, V., Farooq, S., Krantz, W.B.: Design of a two-step pulsed pressure-swing adsorption-based oxygen concentrator. AIChE J. **56**, 354–370 (2010)

Rama Rao, V., Farooq, S.: Experimental study of a pulsed pressure-swing adsorption process with very small 5A zeolite particles for oxygen enrichment. Ind. Eng. Chem. Res. **53**, 13157–13170 (2014a)

Rama Rao, V., Kothare, M.V., Sircar, S.: Numerical simulation of rapid pressurization and depressurization of a zeolite column using nitrogen. Adsorption **20**, 53–60 (2014b)

Rama Rao, V., Chai, S.W., Kothare, M.V., Sircar, S.: Highlights of non-equilibrium, non-isobaric, non-isothermal desorption of nitrogen from a LiX zeolite column by rapid pressure reduction and rapid purge by oxygen. Adsorption **20**, 477–481 (2014c)

Rama Rao, V., Kothare, M.V., Sircar, S.: Novel design and performance of a medical oxygen concentrator using a rapid pressure swing adsorption concept. AIChE J. **60**, 3330–3335 (2014d)

Rama Rao, V., Wu, C.W., Kothare, M.V., Sircar, S.: Comparative performances of two commercial samples of LiLSX zeolite for production of 90% oxygen from air by a novel rapid pressure swing adsorption system. Sep. Sci. Technol. **50**, 1447–1452 (2015)

Rama Rao, V., Kothare, M.V., Sircar, S.: Performance of a medical oxygen concentrator using rapid pressure swing adsorption process: effect of feed air pressure. AIChE J. **62**, 1212–1215 (2016)

Rama Rao, V., Sircar, S.: Comments on reliability of model simulation of rapid pressure swing adsorption process for high-purity product. Ind. Eng. Chem. Res. **56**, 8991–8994 (2017)

Rege, S.U., Yang, R.T.: Limits for air separation by adsorption with LiX zeolite. Ind. Eng. Chem. Res. **36**, 5358–5365 (1997)

Rege, S.U., Yang, R.T.: A simple parameter for selecting an adsorbent for gas separation by pressure swing adsorption. Sep. Sci. Technol. **36**, 3355–3365 (2001)

Reiss, G.: Pressure swing process for the adsorptive separation of gaseous mixtures. US Patent 4,614,525 (1986)

Reiss, G.: Status and development of oxygen generation processes on molecular sieve zeolites. Gas Sep. Purif. **8**, 95–99 (1994)

Rezaei, F., Webley, P.: Optimum structured adsorbents for gas separation processes. Chem. Eng. Sci. **64**, 5182–5191 (2009)

Rota, R., Wankat, P.C.: Intensification of pressure swing adsorption processes. AIChE J. **36**, 1299–1312 (1990)

Rowland, R.O.: Oxygen concentrator. US Patent 4,561,287 (1985)

Ruthven, D.M.: Principles of adsorption and adsorption processes. Wiley, New York (1984)

Ruthven, D.M., Farooq, S., Knaebel, K.S.: Pressure swing adsorption. VCH, New York (1994)

Santos, J.C., Portugal, A.F., Magalhães, F.D., Mendes, A.: Simulation and optimization of small oxygen pressure swing adsorption units. Ind. Eng. Chem. Res. **43**, 8328–8338 (2004)

Santos, J.C., Portugal, A.F., Magalhães, F.D., Mendes, A.: Optimization of medical PSA units for oxygen production. Ind. Eng. Chem. Res. **45**, 1085–1096 (2006)

Santos, J.C., Magalhães, F.D., Mendes, A.: Contamination of zeolites used in oxygen production by PSA: effects of water and carbon dioxide. Ind. Eng. Chem. Res. **47**, 6197–6203 (2008)

Schlaechter, J.: Pressure swing cycle for the separation of oxygen from air. US Patent 4,534,346 (1985)

Shaver, P.R., Schwartz, J., Kirson, D., O-Connor, C.: Emotion knowledge: Further exploration of a prototype approach. J. Pers. Soc. Psychol. **52**, 1061–1086.

Shin, H.S., Kim, D.H., Koo, K.K., Lee, T.S.: Performance of a two-bed pressure swing adsorption process with incomplete pressure equalization. Adsorption **6**, 233–240 (2000)

Sircar, S.: Role of adsorbent heterogeneity on mixed gas adsorption. Ind. Eng. Chem. Res. **29**, 1032 (1991)

Skarstrom, C.W.: Method and apparatus for fractionating gaseous mixtures by adsorption. US Patent 2,944,627 (1960)

Skarstrom, C.W.: Oxygen concentration process. US Patent 3,237,377 (1966)

Smolarek, J., Fassbaugh, J.H., Rogan, M.K., Schaub, H.R.: Vacuum pressure swing adsorption system and method. US Patent 6,010,555 (2000)

Taylor, B., Hansen, P.: Gas concentrator with improved water rejection capability. US Patent 7,780,768 B2 (2010)

Taylor, B., Burgess, P., Hansen, P., Stump, J.: Gas concentrator with removable cartridge adsorbent beds. US Patent 9,592,360 B2 (2017)

Tarpy, S.P., Celli, B.R.: Long-term oxygen therapy. N. Engl. J. Med. **333**, 710–714 (1995)

Todd, R.S., Webley, P.A.: Macropore diffusion dusty-gas coefficient for pelletised zeolites from breakthrough experiments in the O_2/N_2 system. Chem. Eng. Sci. **60**, 4593–4608 (2005)

Todd, R.S., Webley, P.A.: Pressure drop in a packed bed under nonadsorbing and adsorbing conditions. Ind. Eng. Chem. Res. **44**, 7234–7241 (2005)

Wankat, P.C.: Large-scale adsorption and chromatography, vol. 1. CRC Press, Boca Raton (1986)

Wankat, P.C.: Intensification of sorption processes. Ind. Eng. Chem. Res. **26**, 1579–1585 (1987)

Wankat, P.C.: Rate-controlled separations. Elsevier Applied Science, London (1990)

Watson, C.F., Whitley, R.D., Meyer, M.L.: Multiple zeolite adsorbent layers in oxygen separation. US Patent 5,529,610 (1996)

Weston, K., Jaussaud, D., Chiang, R.L.: Lithium exchanged zeolite X adsorbent blends. US Patent 7,300,899 B2 (2007)

Weston, K., Palmore, J., Jaussaud, D.: Zeolite X agglomerates with a halloysite clay binder. US Patent 10,099,201 B1 (2018)

Whitley, R.D., Wagner, G.P., LaBuda, M.J.: Dual mode medical oxygen concentrator. US Patent 7,273,051 B2 (2007)

Whitley, R.D., Wagner, G.P., LaBuda, M.J., Schiff, D.R., Byar, P.D., Weiman, A.M., Wyrick, S.G.: Portable medical oxygen concentrator. US Patent 7,510,601 B2 (2009)

Wilson, S.J., Beh, C.C.K., Webley, P.A., Todd, R.S.: The effects of a readily adsorbed trace component (water) in a bulk separation psa process: the case of oxygen VSA. Ind. Eng. Chem. Res. **40**, 2702–2713 (2001)

Wilson, S.J., Webley, P.A.: Cyclic steady-state axial temperature profiles in multilayer, bulk gas PSA—the case of oxygen VSA. Ind. Eng. Chem. Res. **41**, 2753–2765 (2002)

Wu, C.W., Kothare, M.V., Sircar, S.: Model analysis of equilibrium adsorption isotherms of pure N_2 and O_2 and their binary mixtures on LiLSX zeolite. Ind. Eng. Chem. Res. **53**, 12428–12434 (2014)

Wu, C.W., Kothare, M.V., Sircar, S.: Equilibrium adsorption isotherms of pure N_2 and O_2 and their binary mixtures on LiLSX zeolite: experimental data and thermodynamic analysis. Ind. Eng. Chem. Res. **53**, 7195–7201 (2014)

Wu, C.W., Kothare, M.V., Sircar, S.: Column dynamic study of mass transfer of pure N_2 and O_2 into small particles of pelletized LiLSX zeolite. Ind. Eng. Chem. Res. **53**, 17806–17810 (2014)

Wu, C.W., Kothare, M.V., Sircar, S.: Equilibrium isotherm and mass transfer coefficient for adsorption of pure argon on small particles of pelletized lithium-exchanged low silica X zeolite. Ind. Eng. Chem. Res. **54**, 2385–2390 (2015)

Wu, C.W., Rama Rao, V., Kothare, M.V., Sircar, S.: Experimental study of a novel rapid pressure-swing adsorption based medical oxygen concentrator: effect of the adsorbent selectivity of N_2 over O_2. Ind. Eng. Chem. Res. **55**, 4676–4681 (2016)

Yang, R.T.: Gas separation by adsorption processes. Butterworths, Boston (1987)

Yang, R.T.: Adsorbents: fundamentals and applications. Wiley, New York (2003)

Yon, C.M., Turnock, P.H.: Multicomponent adsorption equilibria on molecular sieves. In: Lee, M.N.Y., Zwiebel, I. (eds.) Adsorption Technology, AIChE Symposium Series v67, no. 117, pp. 75-83, AIChE, New York (1971)

Zheng, J., Barrett, P.A., Pontonio, S.J., Stephenson, N.A., Chandra, P., Kechagia, P.: High-rate and high-density gas separation adsorbents and manufacturing method. Adsorption **20**, 147–156 (2014)

Zheng, X., Yao, H., Huang, Y.: Orthogonal numerical simulation on multi-factor design for rapid pressure swing adsorption. Adsorption **23**, 685–697 (2017)

Zhong, G., Rankin, P.J., Ackley, M.W.: High frequency PSA process for gas separation. US Patent 7,828,878 B2 (2010)

Zhou, S., Chatburn, R.L.: Effect of the anatomic reservoir on low-flow oxygen delivery via nasal cannula: constant flow versus pulse flow with portable oxygen concentrator. Respir Care **59**, 1199–1209 (2014)

Zhu, X., Liu, Y., Yang, X., Liu, W.: Study of a novel rapid vacuum pressure swing adsorption process with intermediate gas pressurization for producing oxygen. Adsorption **23**, 175–184 (2017)